This project has received funding from the European Union's Horizon 2020 research and innovation programme under grant agreement No 952439.

STELLAR
Scientific and Technological Excellence by Leveraging LOFAR Advancements in Radio Astronomy

INSTITUTE OF ASTRONOMY
NATIONAL ASTRONOMICAL OBSERVATORY

Introduction to radio astronomy

Rositsa Miteva
IANAO-BAS
rmiteva@nao-rozhen.org

ASTRON

DIAS
Institiúid Ard-Léinn Bhaile Átha Cliath | Dublin Institute for Advanced Studies

This project has received funding from the European Union's Horizon 2020 research and innovation programme under grant agreement No 952439.

Radio domain:

- from **300 GHz** (~1 THz: IR) to **~30 kHz** (solar wind cutoff)
- ~5 orders of magnitude
- longest wavelengths → **weakest energy** (power output: 10^-15 W needs to be amplified to mW with time integration from sec to many hours)
- to use the wave-like properties of the radio-light: the incoming radio wave electric field generates voltage in conducting wire (antenna)

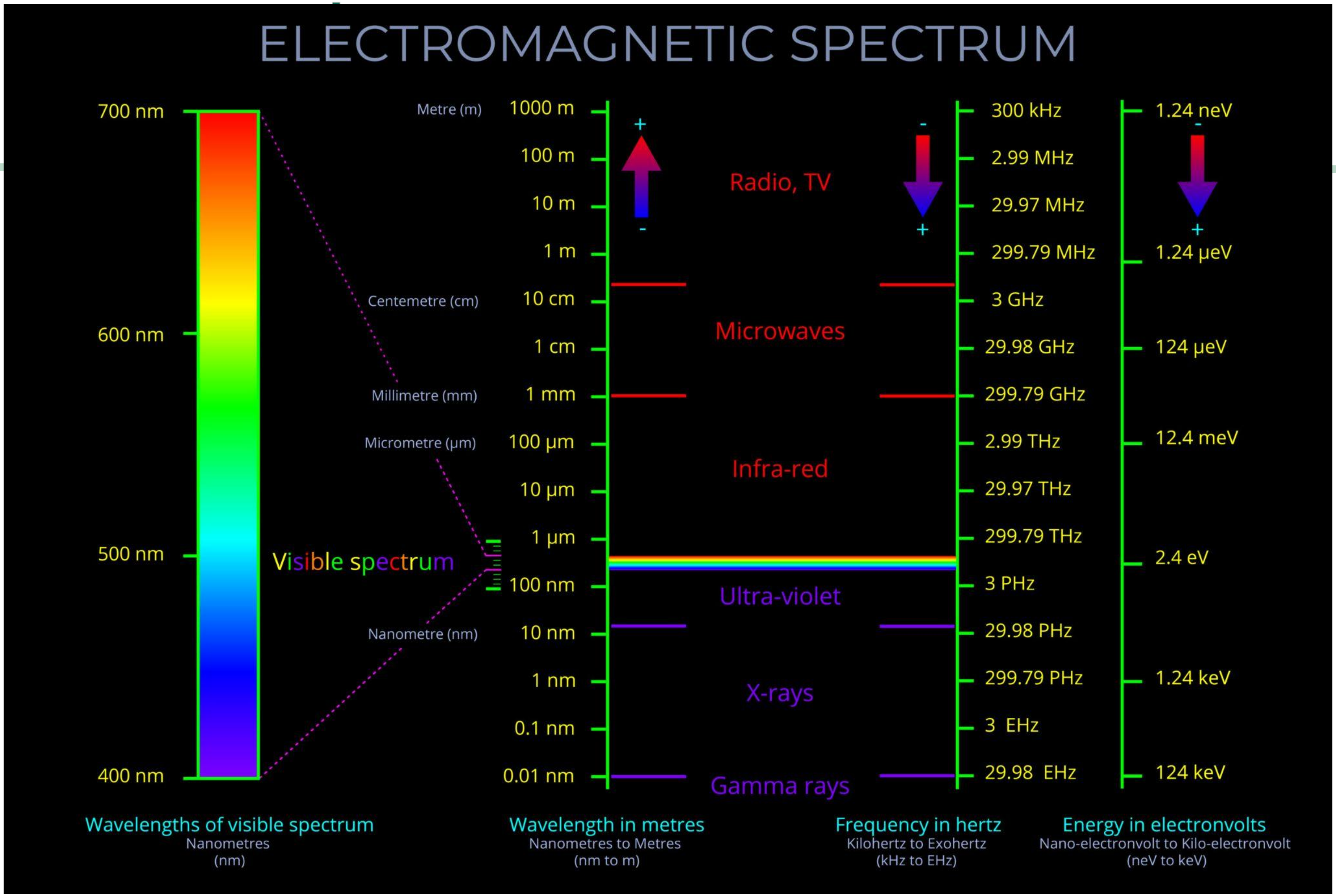

https://lightcolourvision.org/diagrams/electromagnetic-spectrum/

STELLAR
Scientific and Technological Excellence by Leveraging LOFAR Advancements in Radio Astronomy

INSTITUTE OF ASTRONOMY
NATIONAL ASTRONOMICAL OBSERVATORY

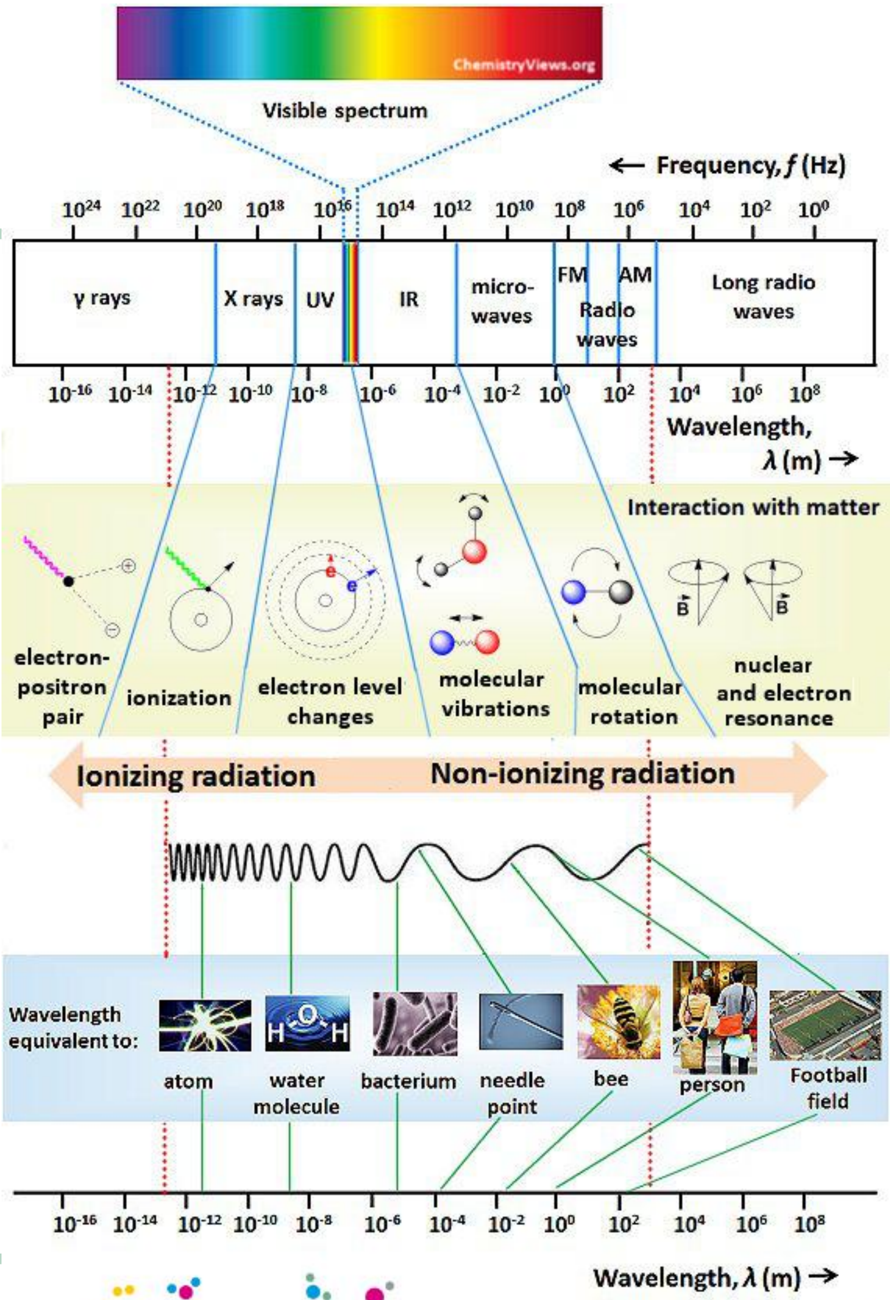

ELECTROMAGNETIC SPECTRUM

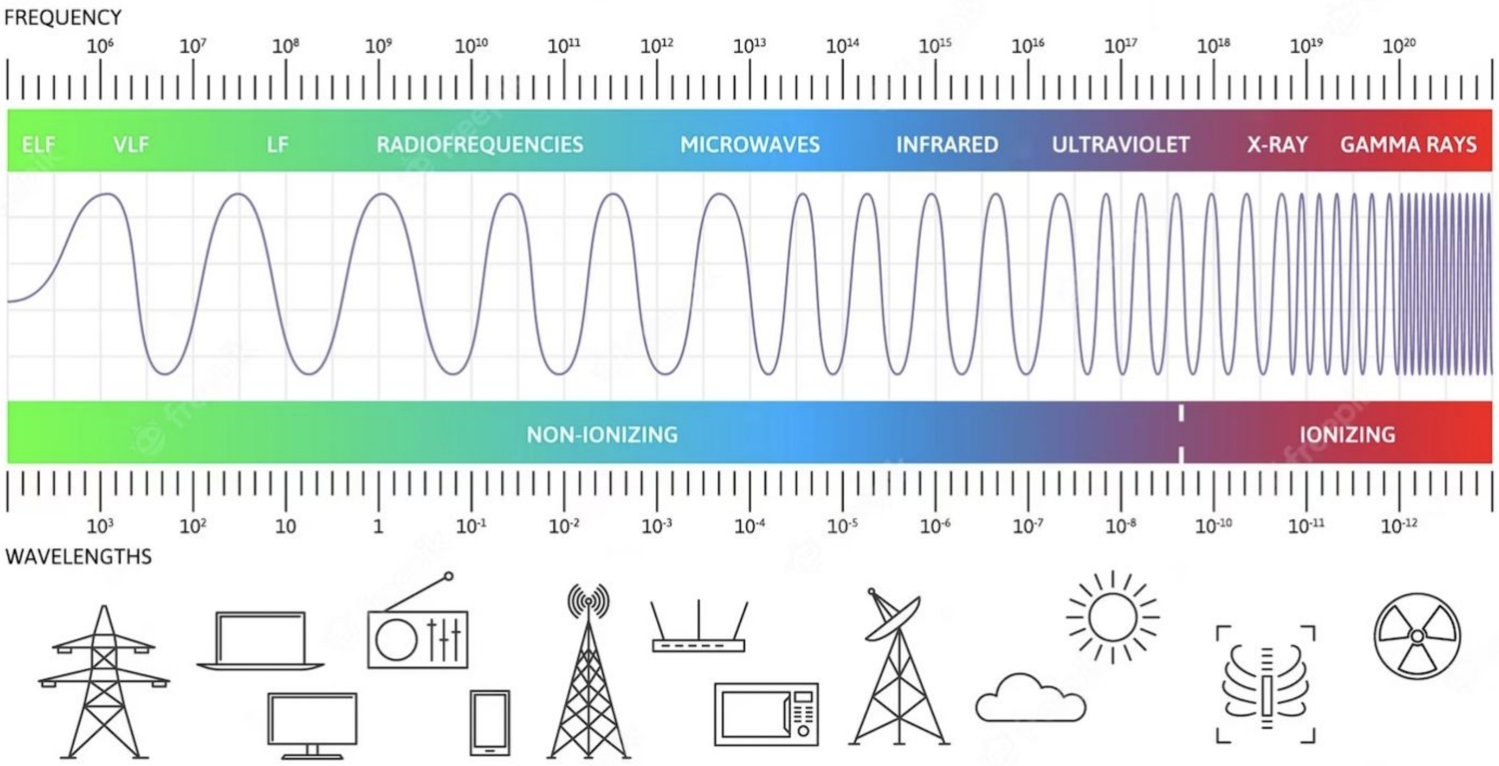

ChemistryViews

https://www.chemistryviews.org/details/ezine/5283841/The_Electromagnetic_Spectrum/

TRON

DIAS
Institiúid Ard-Léinn Bhaile Átha Cliath | Dublin Institute for Advanced Studies

https://www.freepik.com/

This project has received funding from the European Union's Horizon 2020 research and innovation programme under grant agreement No 952439.

STELLAR
Scientific and Technological Excellence by Leveraging LOFAR Advancements in Radio Astronomy

INSTITUTE OF ASTRONOMY NATIONAL ASTRONOMICAL OBSERVATORY

Why radio?

Radio wavelengths are:

- greater than dust particle sizes (dust regions are transparent!)
- greater than water droplets (clouds are transparent!)

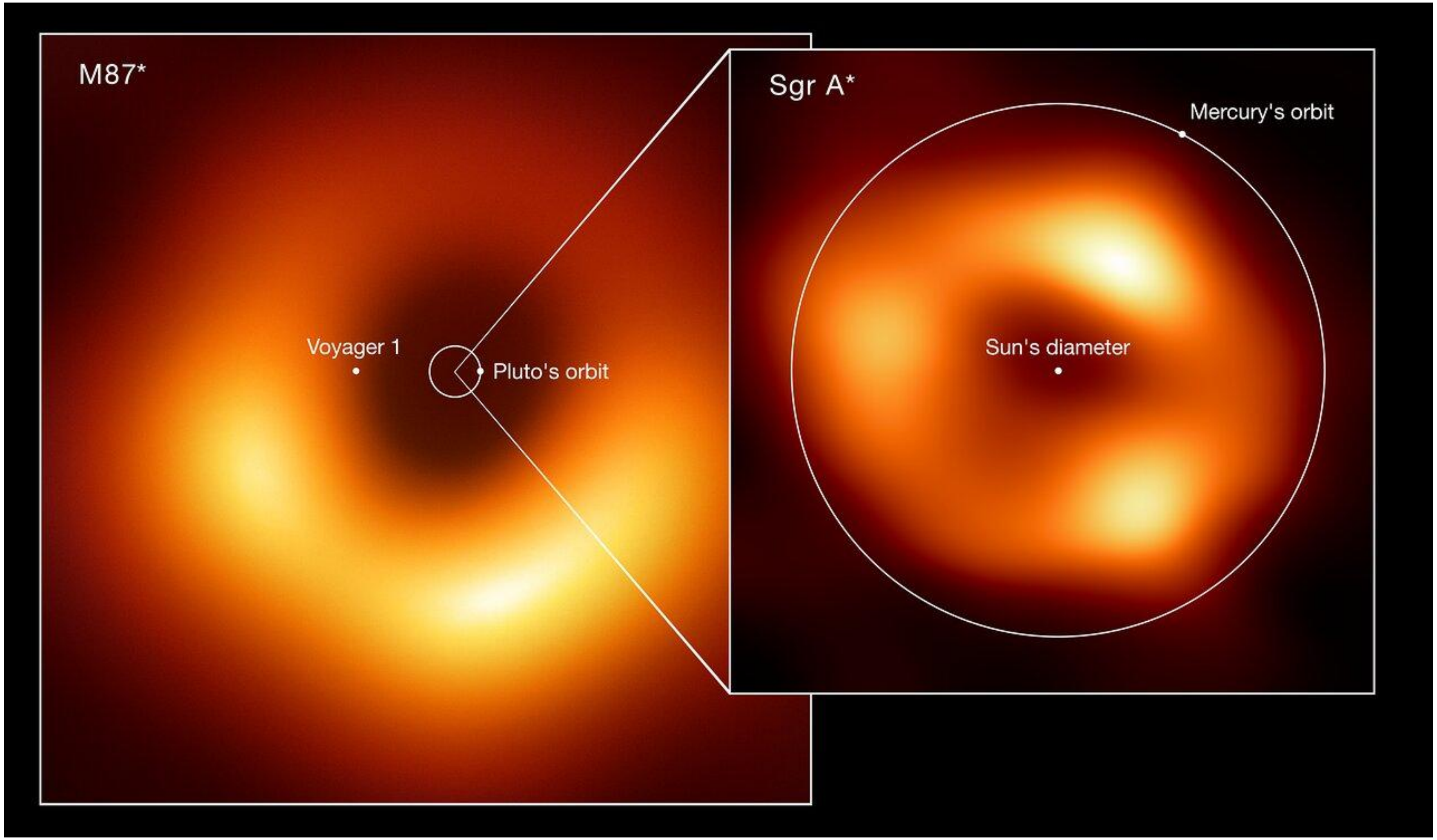

EHT (few-100s GHz),
https://www.eso.org/public/images/eso2208-eht-mwe/

ASTRON

DIAS
Institiúid Ard-Léinn Bhaile Átha Cliath | Dublin Institute for Advanced Studies

This project has received funding from the European Union's Horizon 2020 research and innovation programme under grant agreement No 952439.

STELLAR
Scientific and Technological Excellence by Leveraging LOFAR Advancements in Radio Astronomy

INSTITUTE OF ASTRONOMY
NATIONAL ASTRONOMICAL OBSERVATORY

(Pre-)history of radio astronomy

1785: Coulomb - electrostatics
Bio-Savart - B-field generated by electric current
1819: Oersted - electricity produces magnetism
1825: Ampere - force law, magnetostatics
1831: Faraday - magnetism produces electricity
1834: Lenz - on direction of induction
1846: Neumann - on induced force by magnetic field

Name	**Integral** equations	**Differential** equations
Gauss's law	$\oiint_{\partial\Omega} \mathbf{E}\cdot d\mathbf{S} = \frac{1}{\varepsilon_0}\iiint_\Omega \rho\, dV$	$\nabla\cdot\mathbf{E} = \frac{\rho}{\varepsilon_0}$
Gauss's law for magnetism	$\oiint_{\partial\Omega} \mathbf{B}\cdot d\mathbf{S} = 0$	$\nabla\cdot\mathbf{B} = 0$
Maxwell–Faraday equation (Faraday's law of induction)	$\oint_{\partial\Sigma} \mathbf{E}\cdot d\boldsymbol{\ell} = -\frac{d}{dt}\iint_\Sigma \mathbf{B}\cdot d\mathbf{S}$	$\nabla\times\mathbf{E} = -\frac{\partial \mathbf{B}}{\partial t}$
Ampère's circuital law (with Maxwell's addition)	$\oint_{\partial\Sigma} \mathbf{B}\cdot d\boldsymbol{\ell} = \mu_0\left(\iint_\Sigma \mathbf{J}\cdot d\mathbf{S} + \varepsilon_0\frac{d}{dt}\iint_\Sigma \mathbf{E}\cdot d\mathbf{S}\right)$	$\nabla\times\mathbf{B} = \mu_0\left(\mathbf{J} + \varepsilon_0\frac{\partial \mathbf{E}}{\partial t}\right)$

1864

James Maxwell

1886

Heinrich Hertz

"I do not think that the wireless waves I have discovered will have any practical application."

unit of frequency: cycles/sec == Hz

~1900

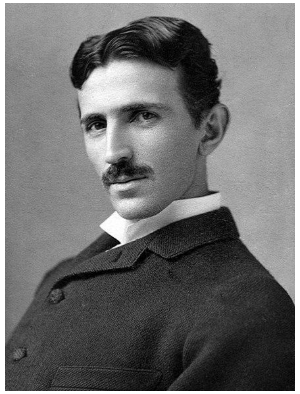

Nikola Tesla

- Dolbear
- Branly
- Lodge
- Tesla
- Popoff
- Marconi
- Slaby
- Fessenden
- De Forest, etc.

The Nobel Prize in Physics 1909

Photo from the Nobel Foundation archive.
Guglielmo Marconi
Prize share: 1/2

Photo from the Nobel Foundation archive.
Karl Ferdinand Braun
Prize share: 1/2

The Nobel Prize in Physics 1909 was awarded jointly to Guglielmo Marconi and Karl Ferdinand Braun "in recognition of their contributions to the development of wireless telegraphy"

https://www.nobelprize.org/prizes/physics/1909/summary/

https://en.wikipedia.org/

ASTRON

DIAS
Institiúid Ard-Léinn Bhaile Átha Cliath | Dublin Institute for Advanced Studies

This project has received funding from the European Union's Horizon 2020 research and innovation programme under grant agreement No 952439.

STELLAR
Scientific and Technological Excellence by Leveraging LOFAR Advancements in Radio Astronomy

INSTITUTE OF ASTRONOMY NATIONAL ASTRONOMICAL OBSERVATORY

https://suli.pppl.gov/2021/course/IntroToPlasma_Matthews2021.pdf

$$\nabla \cdot \vec{E} = \frac{\rho}{\epsilon_0}$$

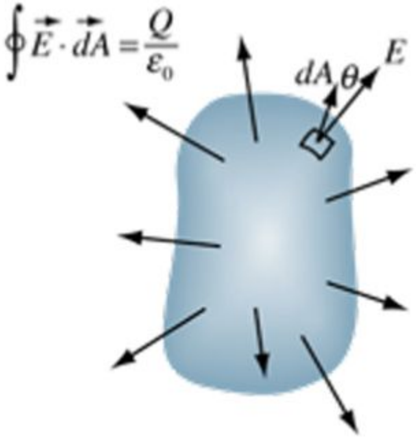

$$\nabla \times \vec{B} = \mu_0 \vec{J} + \frac{1}{c^2}\frac{d\vec{E}}{dt}$$

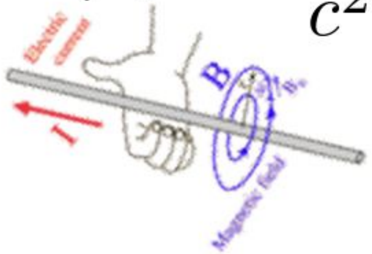

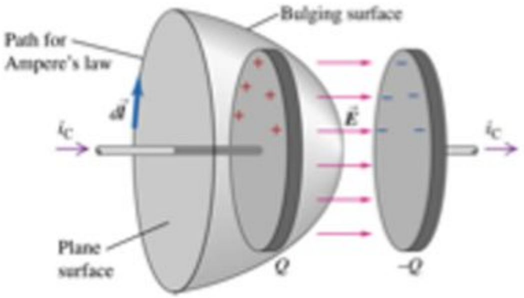

$$\nabla \times \vec{E} = -\frac{d\vec{B}}{dt}$$

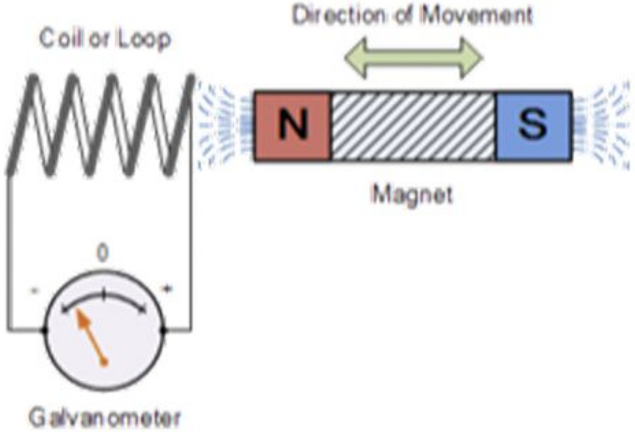

$$\nabla \cdot \vec{B} = 0$$

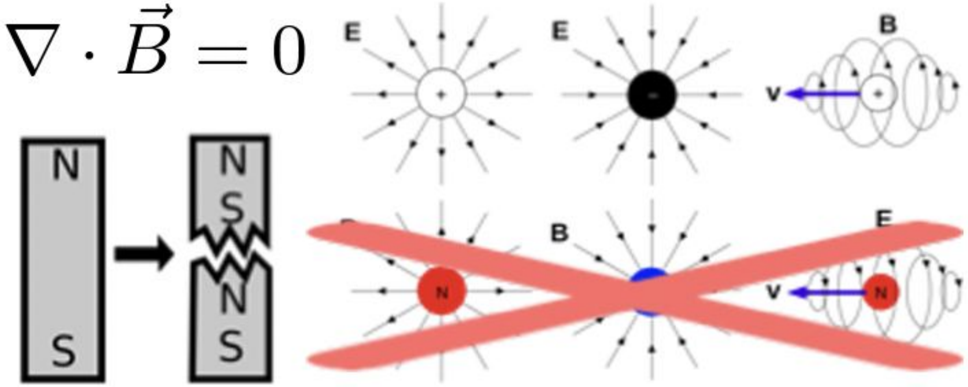

This project has received funding from the European Union's Horizon 2020 research and innovation programme under grant agreement No 952439.

STELLAR
Scientific and Technological Excellence by Leveraging LOFAR Advancements in Radio Astronomy

Radio wave propagation (McKean lecture notes, 2022)

$$\nabla \times (\nabla \times \vec{E}) = \frac{d}{dt}(\nabla \times \vec{B}) = \mu_0 \sigma \dot{\vec{E}} + \mu_0 \epsilon_0 \ddot{\vec{E}}$$

$$E(r,t) = E_0 e^{-i(wt-kr)}$$

$$\vec{J} = \sigma \vec{E}$$

Conductivity

$$m_e \dot{v} = -e\,\vec{E}(r,t)$$

$$c = \frac{1}{\sqrt{\mu_0 \epsilon_0}}$$

permeability permittivity

$$k^2 = \frac{\omega^2}{c^2}\left(1 - \frac{\omega_p^2}{\omega^2}\right)$$ where $$\omega_p = \sqrt{\frac{n_e e^2}{\epsilon_0 m_e}}$$

$$f_{\rm pe} = \frac{\omega_{\rm pe}}{2\pi}\ [\mathrm{Hz}]$$

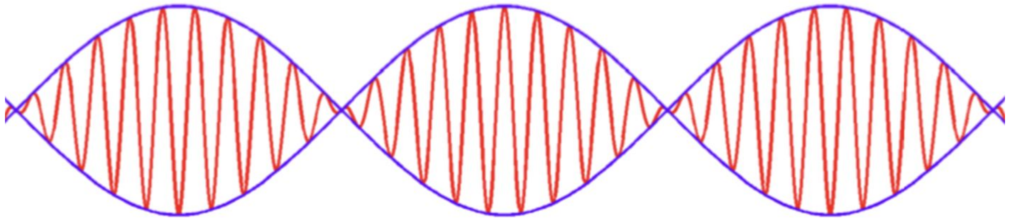

$$v_p = \frac{c}{\sqrt{\left(1 - \frac{\omega_p^2}{\omega^2}\right)}}$$

$$v_g = c\sqrt{1 - \frac{\omega_p^2}{\omega^2}}$$

$$n = \sqrt{1 - \frac{\omega_p^2}{\omega^2}}$$

This project has received funding from the European Union's Horizon 2020 research and innovation programme under grant agreement No 952439.

STELLAR
Scientific and Technological Excellence by Leveraging LOFAR Advancements in Radio Astronomy

(McKean lecture notes, 2022)

Worked example: What is the cut-off frequency for LOFAR observations carried out when the electron density is $N_e = 2.5 \times 10^5$ cm^{-3} (night time) and $N_e = 1.5 \times 10^6$ cm^{-3} (day time)?

$$\nu_\mathrm{p}[\mathrm{Hz}] = 8.97 \times 10^3 \sqrt{\frac{2.5 \times 10^5}{[\mathrm{cm}^{-3}]}} = 4.5\ \mathrm{MHz} \qquad \text{(night time)}$$

$$\nu_\mathrm{p}[\mathrm{Hz}] = 8.97 \times 10^3 \sqrt{\frac{1.5 \times 10^6}{[\mathrm{cm}^{-3}]}} = 11\ \mathrm{MHz} \qquad \text{(day time)}$$

$$f_{pe} = \omega_{pe}/2\pi = 8.98 \times 10^3 n_e{}^{1/2}\ \mathrm{Hz}$$

- At frequencies,
  1. $\omega < \omega_\mathrm{p}$: n^2 is negative, reflection (ν < 10 MHz),
  2. $\omega > \omega_\mathrm{p}$: n^2 is positive, refraction (10 MHz < ν < 10 GHz),
  3. $\omega \gg \omega_\mathrm{p}$: n^2 is unity (ν > 10 GHz).

This project has received funding from the European Union's Horizon 2020 research and innovation programme under grant agreement No 952439.

STELLAR
Scientific and Technological Excellence by Leveraging LOFAR Advancements in Radio Astronomy

INSTITUTE OF ASTRONOMY NATIONAL ASTRONOMICAL OBSERVATORY

Limitations for the radio observations

reflection, absorption (scintillations) by the **Earth's ionosphere** (ionozation due to solar X-ray and EUV emission)

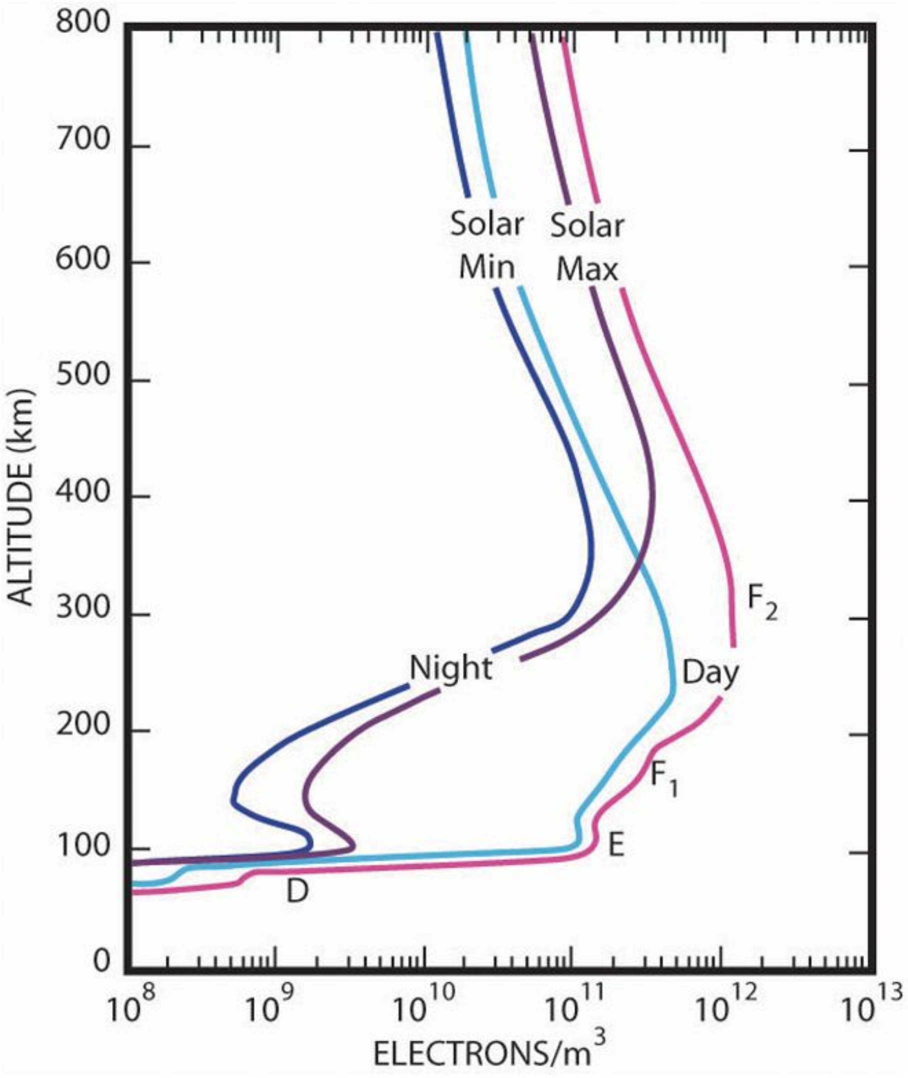

Aikio, 2011, www.sgo.fi

Ionospheric regions and typical daytime electron densities:

- D region: 60–90 km, $n_e = 10^8$–10^{10} m^{-3}
- E region: 90–150 km, $n_e = 10^{10}$–10^{11} m^{-3}
- F region: 150–1000 km, $n_e = 10^{11}$–10^{12} m^{-3} .

Ionosphere has great variability:

- Solar cycle variations (in specific upper F region)
- Day-night variation in lower F, E and D regions
- Space weather effects based on short-term solar variability (lower F, E and D regions)

This project has received funding from the European Union's Horizon 2020 research and innovation programme under grant agreement No 952439.

STELLAR
Scientific and Technological Excellence by Leveraging LOFAR Advancements in Radio Astronomy

Limitations for the radio observations: low-frequency limit (MHz)

Reflections and refraction (bending) depends on:

- ionospheric density
- wave frequency
- angle of incidence

F2 layer primarily reflects the radio waves

kHz waves: only with satellites

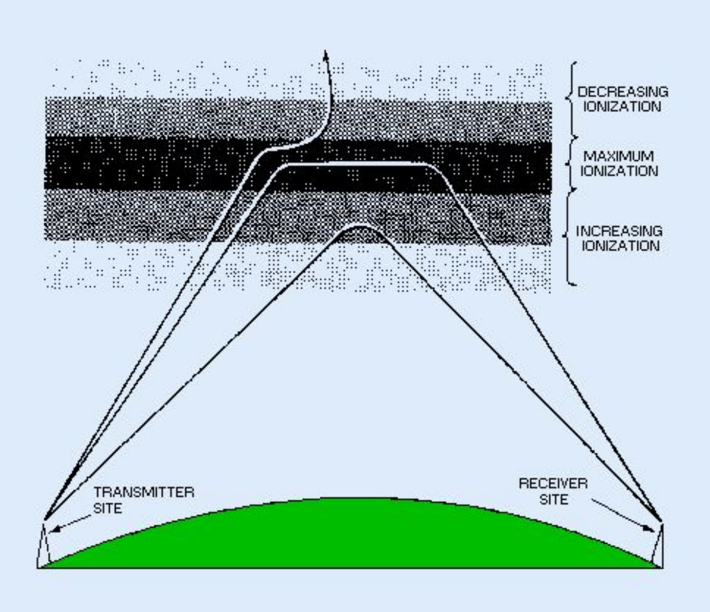

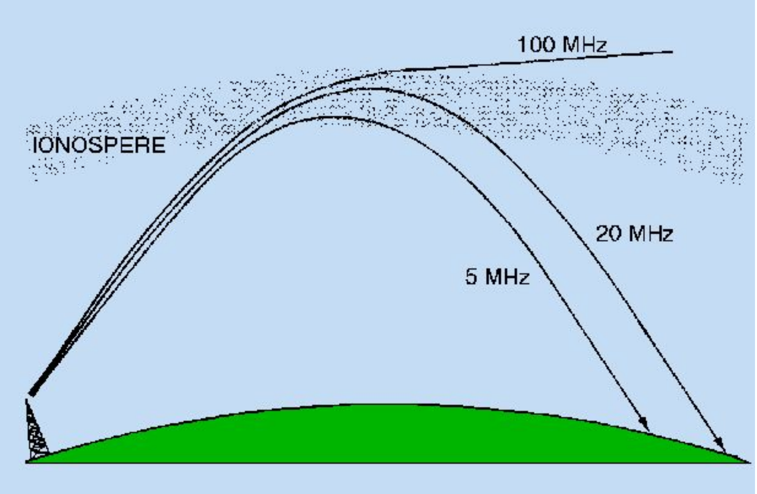

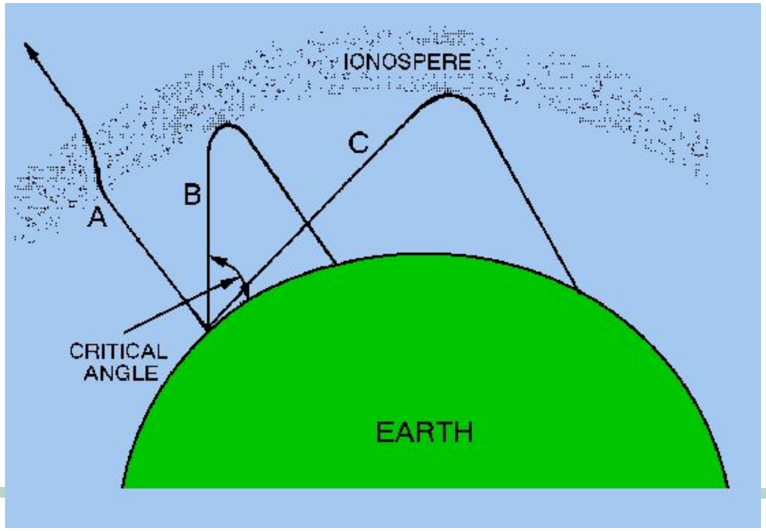

http://www.tpub.com/neets/book10/40e.htm

This project has received funding from the European Union's Horizon 2020 research and innovation programme under grant agreement No 952439.

STELLAR
Scientific and Technological Excellence by Leveraging LOFAR Advancements in Radio Astronomy

Limitations for the radio observations: high-frequency limit (GHz)

- Optical depth (τ): A measure of the absorption / scattering (attenuation) of electromagnetic radiation in a medium (probability of an interaction),

$$\tau_i(\lambda, z_0) = \int_{z_0}^{\infty} n_i(z)\,\sigma\,dz = \int_{z_0}^{\infty} r_i(z)\,\rho_0(z)\,k_i(\lambda)\,dz$$

or, in terms of the linear absorption co-efficient (κ),

$$\tau_i(\lambda, z_0) = \int_{z_0}^{\infty} \kappa(\lambda, z)\,dz \qquad \text{where} \quad \kappa(\lambda, z) = k_i(\lambda)\,\rho_i(z)$$

linear absorption co-efficient (cm^{-1})

Mass density of species i (g cm^{-3})

Mass attenuation co-efficient (cm^2 g^{-1})

$$k_i = \frac{\sigma\,n_i}{r_i\,\rho_0}$$

Cross-section (cm^2)

Number density of particles (cm^{-3})

Mass attenuation co-efficient (cm^2 g^{-1})

Mixing ratio (= ρ_i/ρ_0)

Mass density of air (g cm^{-3})

The attenuation of an incident ray of intensity I_0, received at altitude z_0, summed over all absorbing species is,

$$I(z_0) = I_0 \exp\left[-\sum_i \tau(\lambda, z_0)\right] = I_0 \exp\left[-\tau(z)\right] \qquad \tau = -\ln\left(\frac{I(z_0)}{I_0}\right)$$

τ = 2.3 x Attenuation

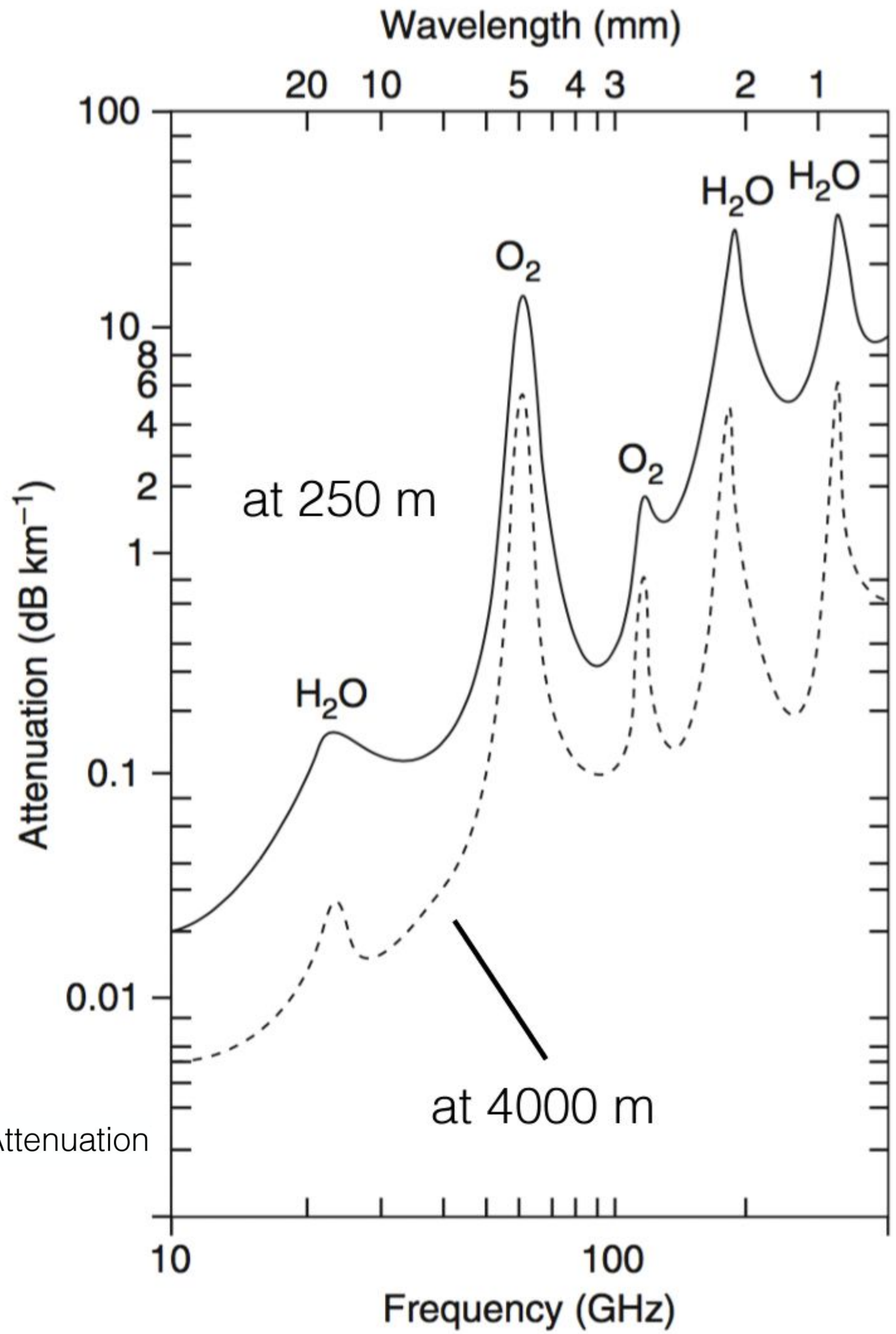

(McKean lecture notes, 2022)

ASTRON

This project has received funding from the European Union's Horizon 2020 research and innovation programme under grant agreement No 952439.

STELLAR
Scientific and Technological Excellence by Leveraging LOFAR Advancements in Radio Astronomy

Summary on observing windows:
Earth's atmosphere is transparent from few GHz (cm-wave) - few MHz (m-wave)

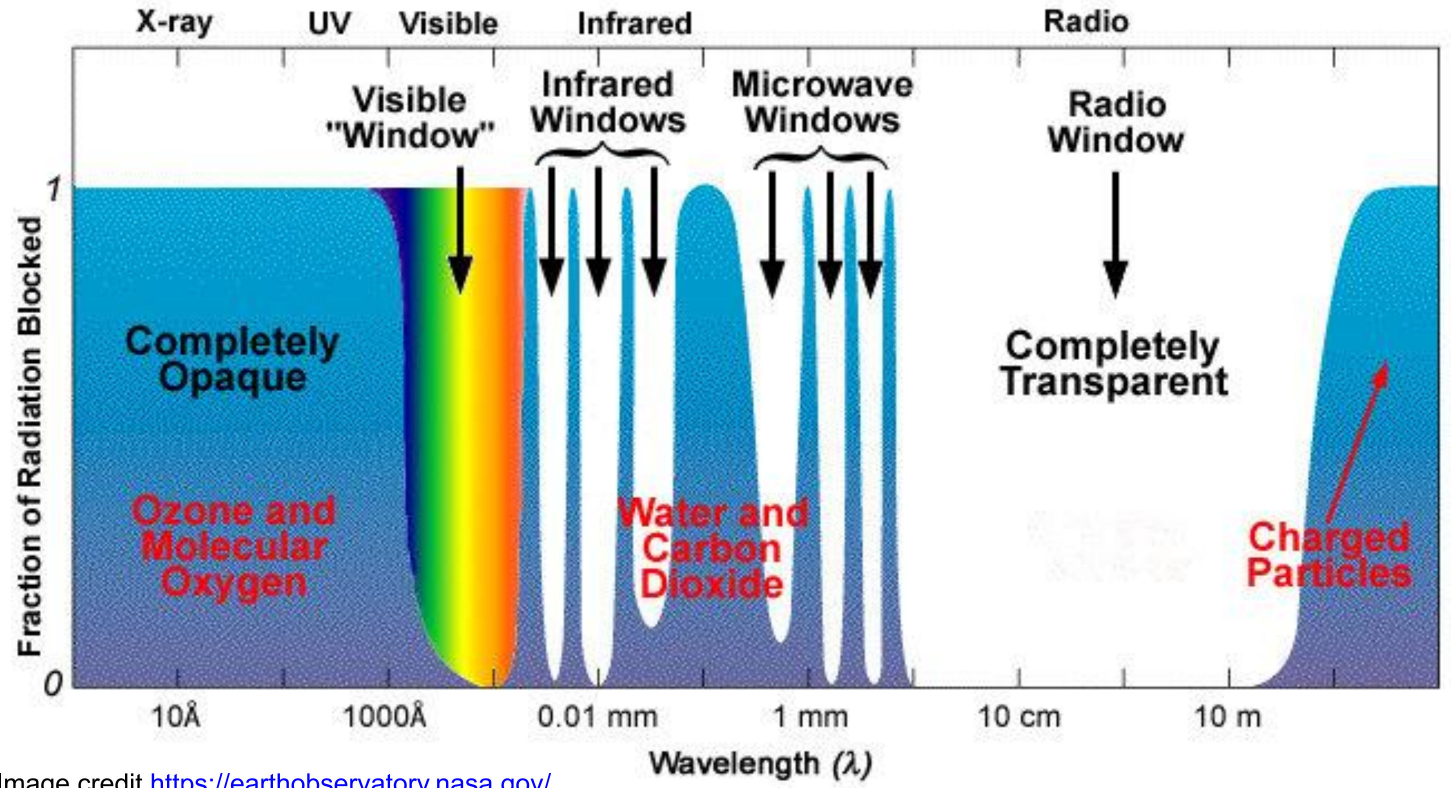

Image credit https://earthobservatory.nasa.gov/

300 GHz 3 GHz 30 MHz

submm-mm/IR-MW:
H2O (~22 GHz) & O2 (52-60 GHz)-absorption
- ALMA: 31-1000 GHz
- VLA: 1-50 GHz
- e-MERLIN: 1.4, 5, 6, 22 GHz

high altitudes (> 4000 m)
dry places

m/MHz: radio window

km/kHz-range: Ionospheric reflection

This project has received funding from the European Union's Horizon 2020 research and innovation programme under grant agreement No 952439.

Issues for radio astronomy

- Black-body emission has very low intensity @ radio
- low sensitivity of the receivers

Non-detections

- 1895: Oliver Lodge (Sun); proposed to move to isolated places to avoid man-made interference
- Thomas Edison (Sun)
- Nikola Tesla (planets)
- 1933: Artur Adel & John Kraus (Sun), cm-waves

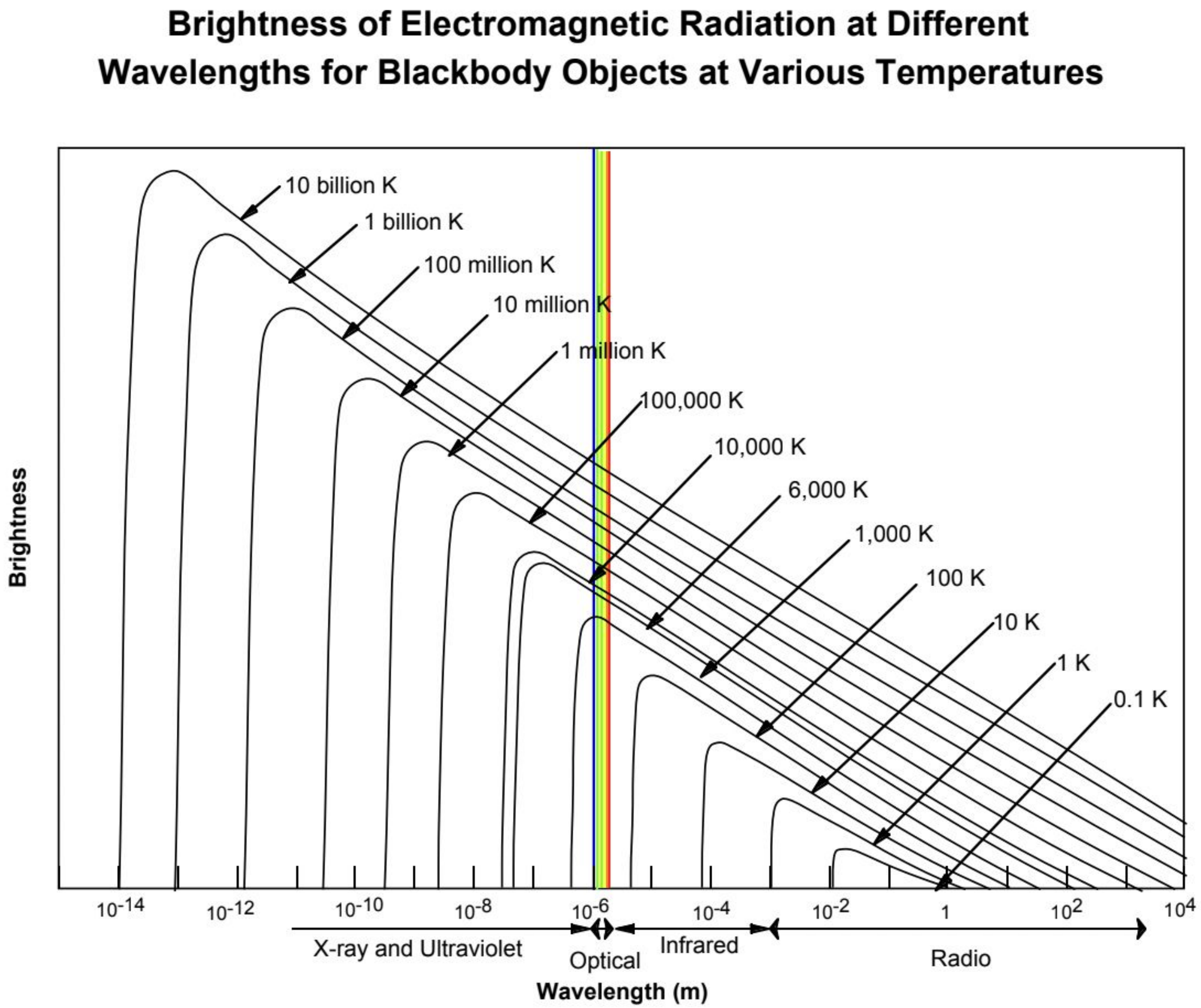

Radio spectrum (Miller, 1995, https://www2.jpl.nasa.gov/radioastronomy/)

This project has received funding from the European Union's Horizon 2020 research and innovation programme under grant agreement No 952439.

Terrestrial radio emissions

- pre-1920: <100 kHz
- ~1920: shift to 1.5 MHz
- post-1920: 10s of MHz (more voice channels, less affected by the ionosphere and thunderstorms)

~1920: AM (amplitude modulation): few kHz - few MHz; subject to radio frequency interference (RFI); ionospheric bounce

after WWII: FM (frequency modulation): ~(60)90-110 MHz; line-of-sight broadcast/detection

~2000: Digital wireless radio & TV: GHz (S-band)

after 1980: Satellite TV (GEO satellites):
Ku, C-bands

Band designation	Frequency range	Explanation of meaning of letters
HF	0.003 to 0.03 GHz	High Frequency
VHF	0.03 to 0.3 GHz	Very High Frequency
UHF	0.3 to 1 GHz	Ultra High Frequency
L	1 to 2 GHz	Long wave
S	2 to 4 GHz	Short wave
C	4 to 8 GHz	Compromise between S and X
X	8 to 12 GHz	Used in WW II for fire control, X for cross (as in crosshair). Exotic.
Ku	12 to 18 GHz	Kurz-under
K	18 to 27 GHz	Kurz (German for “short”)
Ka	27 to 40 GHz	Kurz-above
V	40 to 75 GHz	
W	75 to 110 GHz	W follows V in the alphabet
mm or G	110 to 300 GHz	Millimeter

https://terasense.com/terahertz-technology/radio-frequency-bands/

This project has received funding from the European Union's Horizon 2020 research and innovation programme under grant agreement No 952439.

STELLAR
Scientific and Technological Excellence by Leveraging LOFAR Advancements in Radio Astronomy

INSTITUTE OF ASTRONOMY
NATIONAL ASTRONOMICAL OBSERVATORY

History of radio astronomy: **Karl Guthe Jansky**
Bell Labs: to investigate the static sources (atmospheric and ionospheric interference using 10-20 m radio signals) in trans-Atlantic telephone communications

~30 m diameter antenna
20.5 MHz (14.6 m)

detected statics from local & distant thunderstorms

1931-1933: discovery of radio signal with period 1 sidereal day:
correct identification of the origin - Sagittarius A/Milky way center
unit for intensity (flux density): Jy

$$1\,\mathrm{Jy} = 10^{-26}\,\frac{\mathrm{W}}{\mathrm{Hz}\cdot\mathrm{m}^2} = 10^{-26}\,\frac{\mathrm{J}}{\mathrm{s}\cdot\mathrm{Hz}\cdot\mathrm{m}^2} = 10^{-23}\,\frac{\mathrm{erg}}{\mathrm{s}\cdot\mathrm{Hz}\cdot\mathrm{cm}^2}$$

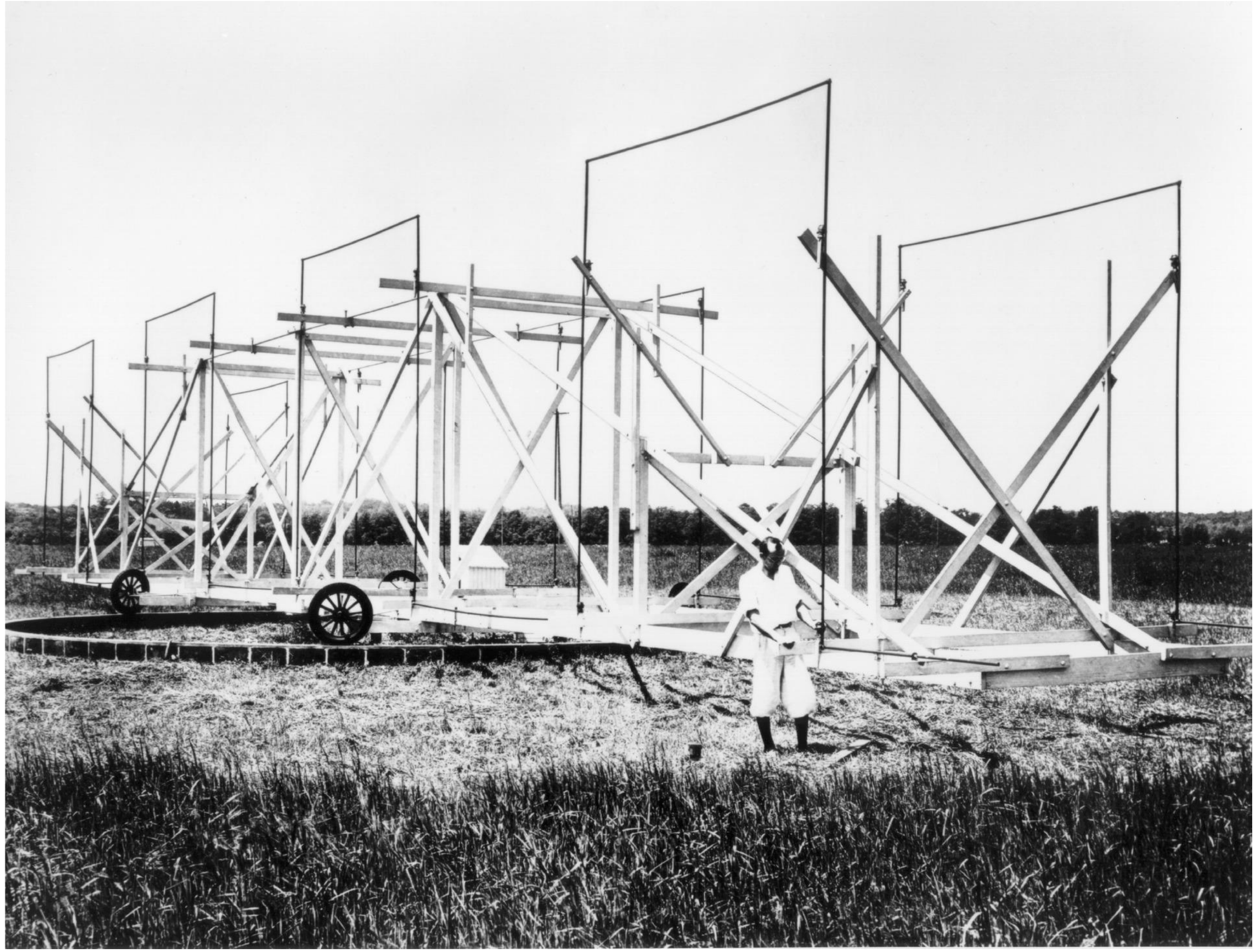

publications:
https://www.nrao.edu/archives/items/show/772

Credit: https://en.wikipedia.org/

DIAS
Institiúid Ard-Léinn Bhaile Átha Cliath | Dublin Institute for Advanced Studies

This project has received funding from the European Union's Horizon 2020 research and innovation programme under grant agreement No 952439.

STELLAR
Scientific and Technological Excellence by Leveraging LOFAR Advancements in Radio Astronomy

History of radio astronomy: **Grote Reber**
1937: builds 9 m dish radio telescope
non-detection: 3.3 GHz, 900 MHz
(confirms the spectrum is not black-body)
detection: 160 MHz
1941-1943: contour maps of Milky way with Cygnus A, Cassiopeia A
publications in ApJ

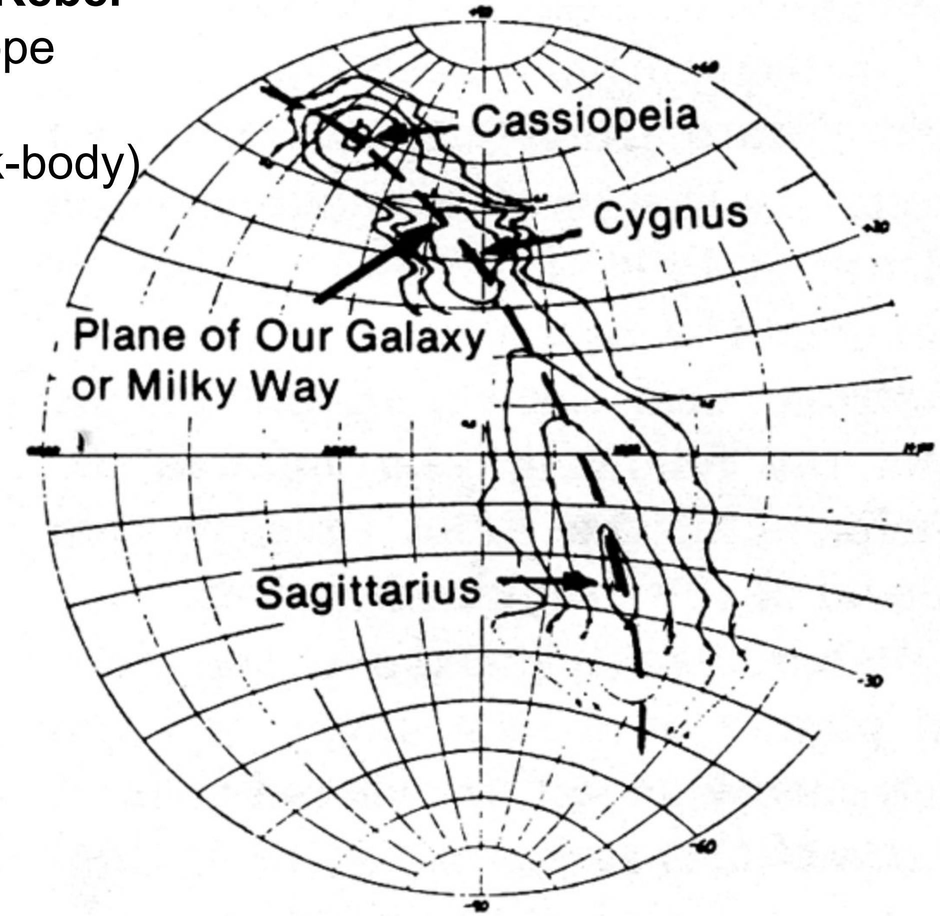

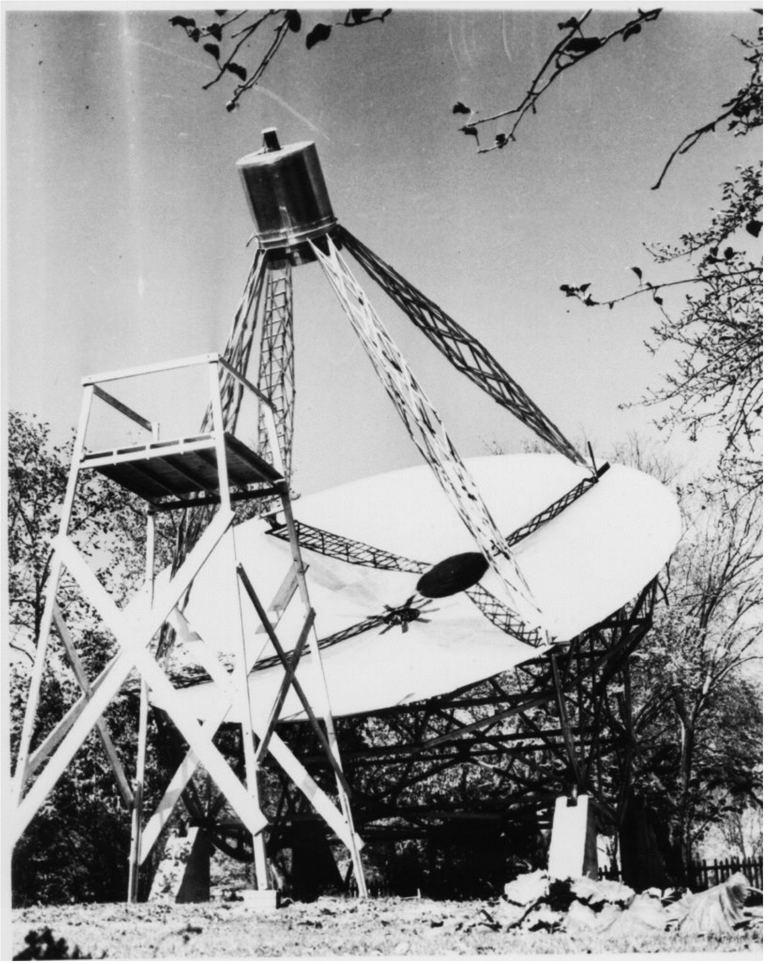

Credit: https://en.wikipedia.org/

This project has received funding from the European Union's Horizon 2020 research and innovation programme under grant agreement No 952439.

A-team (used for callibration)

brightest extra-solar radio sources:

- Saggitarius A - SMBH/Milky way @ 26.7 Kly
- Cassiopeia A - supernova remnant (SNR) @11 Kly
- Cygnus A - radio galaxy @ 756 Mly
- Taurus A (M1) - SNR in Crab nebula
- Virgo A (M87 or NGC 4486) - supergiant radio galaxy @ 16 Mly
- Centaurus A - radio galaxy @ 12 MLy
- Hercules A (3C 348) - radio galaxy @ 2 Bly
- Fornax A - radio galaxy @ 60 Mly
- Hydra A (3C 218) - radio galaxy @ 840 Mly
- Pictor A - radio galaxy @ 485 Mly
- Pupis A - SNR @ 7 Kly

https://research.csiro.au/racs/home/gallery/a-sources/

This project has received funding from the European Union's Horizon 2020 research and innovation programme under grant agreement No 952439.

STELLAR
Scientific and Technological Excellence by Leveraging LOFAR Advancements in Radio Astronomy

History of radio astronomy (post WWII)
UK: Jodrell Bank,

James Hey
1942: discovery of the radio Sun
localized the extra-glalctic origin of Cygnus A

Martin Ryle
1946: first multi-element interferometer
1959: 3C (Cambridge) radio sources catalog published
introduces the Earth-aperture syntesis

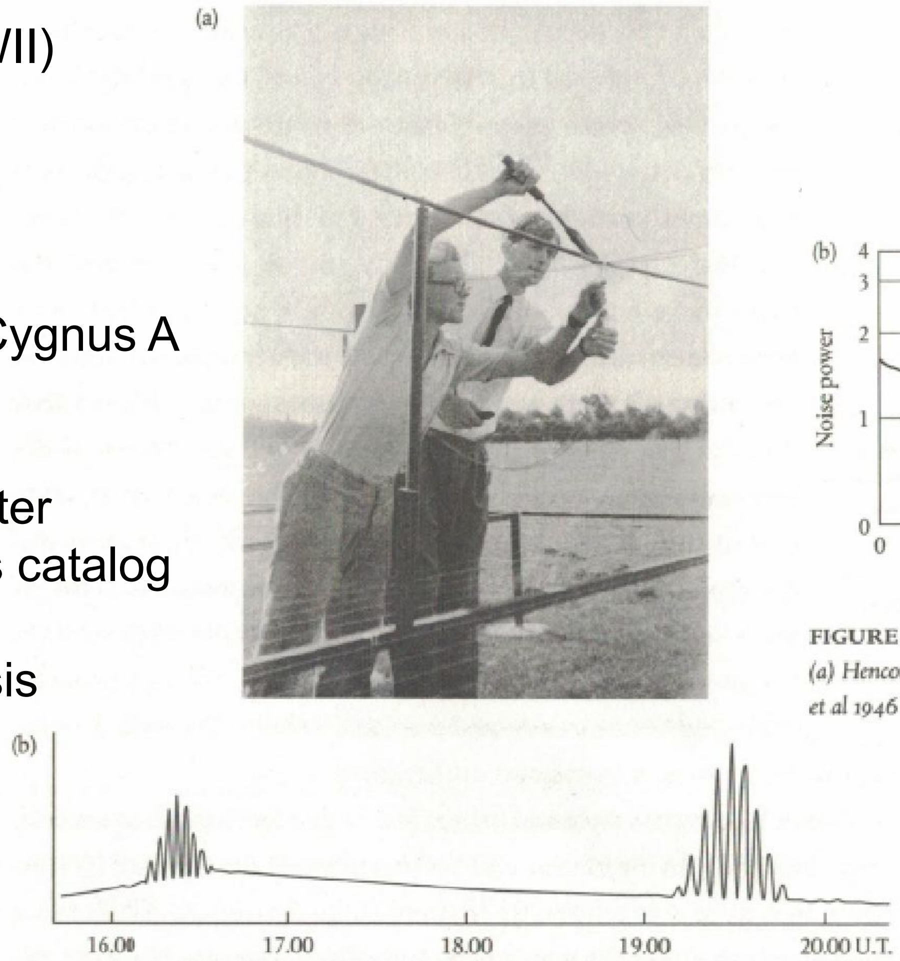

FIGURE 30 (a) Martin Ryle and the author are shown constructing the interferometer antenna. (b) The radio sources Cygnus A and Cassiopeia A recorded with an interferometer at Cambridge in 1949. *(a) Bruce Elsmore. b) Courtesy of Oxford University Press and the Monthly Notices of the Royal Astronomical Society.*

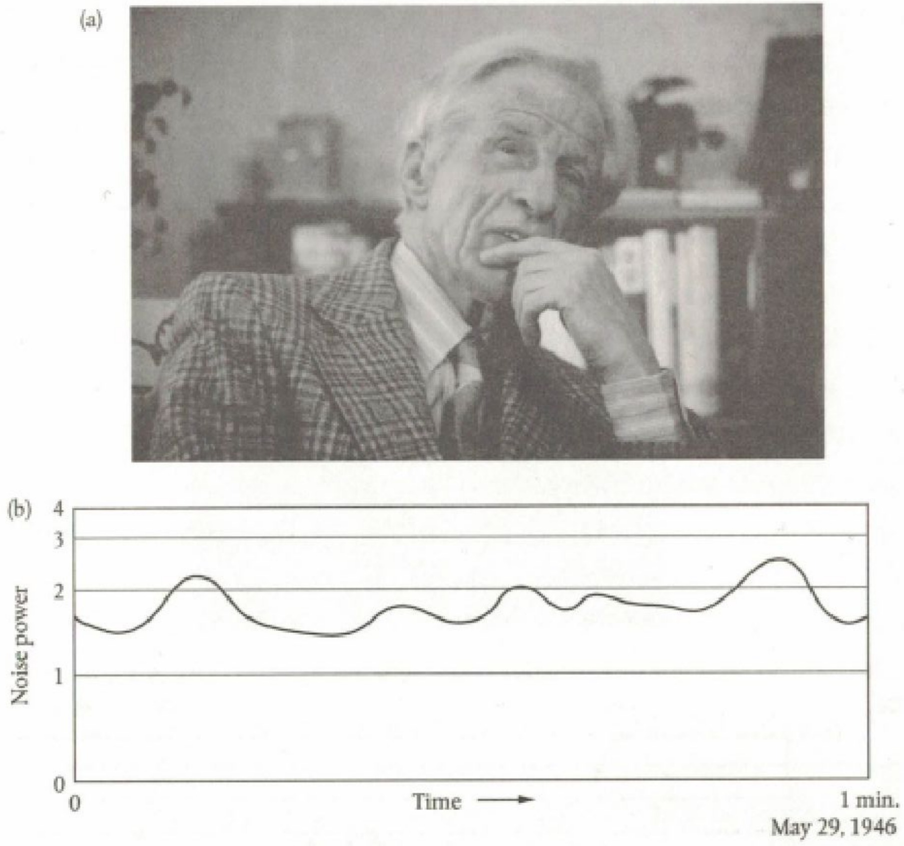

FIGURE 28 James Hey (a) and the record of a fluctuating signal from Cygnus (b). *(a) Hencoup/Galaxy. (b) Reprinted by permission from Macmillan Publishers Ltd: Nature Hey, J.S. et al 1946 'Fluctuations in Cosmic Radiation at Radio-Frequencies' vol. 158 © 1946.*

Credit:
Unseen cosmos

This project has received funding from the European Union's Horizon 2020 research and innovation programme under grant agreement No 952439.

STELLAR

Scientific and Technological Excellence by Leveraging LOFAR Advancements in Radio Astronomy

History of radio astronomy: **‘sea interferometer’** near Sydney, Australia

Joseph Pawsey
early ionospheric irregularities

John Bolton
1948: sunspot observations in radio
detects optical counterparts to:
Cygnus A
Taurus A
Centaurus A

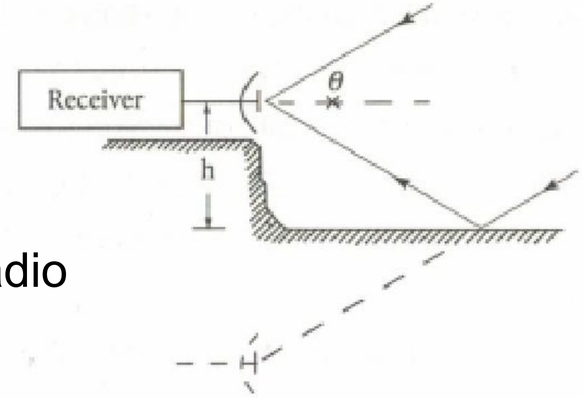

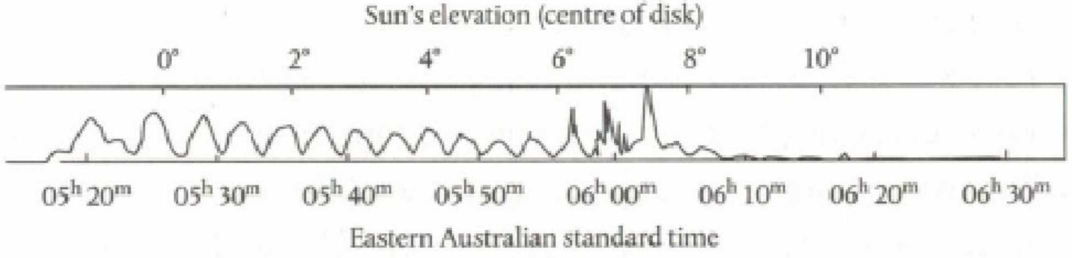

FIGURE 11 Distribution of radio brightness across the Sun: (a) at a long wavelength (2.5 m, 120 MHz), where the corona dominates; (b) at a short wavelength (9 mm, 33 GHz), where the inner part of the corona is seen brightly at the edge of the chromosphere.

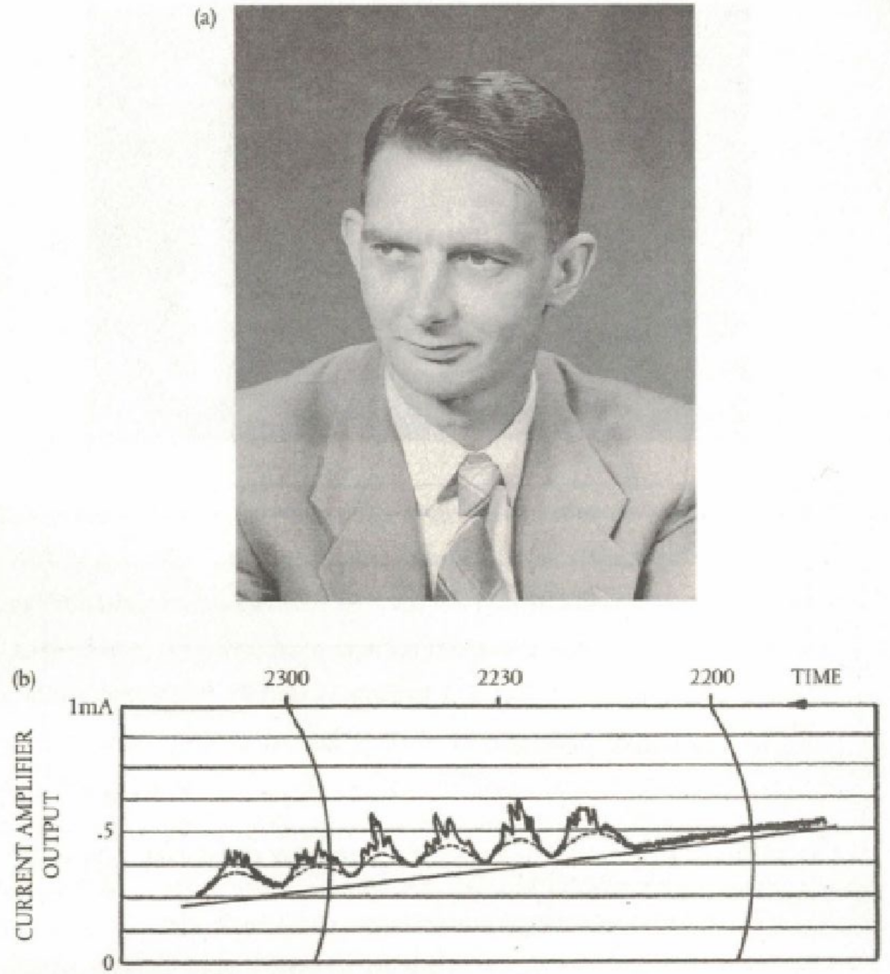

FIGURE 29 John Bolton (a) and the first interferometer record of Cygnus A (b). His interferometer used a single antenna, mounted on a cliff (Dover Heights) near Sydney. Pointing near the horizon, the antenna picked up radio waves reflected in the sea, giving the effect of an interferometer pair spaced by twice the cliff height. Cygnus A rose above the horizon at 2215 (time increases right to left). *(a) Courtesy of the Archives, California Institute of Technology. (b) CSIRO Radio Astronomy Image Archive.*

Credit: Unseen cosmos

This project has received funding from the European Union's Horizon 2020 research and innovation programme under grant agreement No 952439.

Scientific and Technolog Advancem

History of radio astronomy: **21-cm line (1.42 GHz)** diagnostic for HI regions
1944: Hendrik van de Hulst predicts the line upon Jan Oort's task; discovery of the spiral strcture of Milky way
1951: first detection (USA); 3 publications of results: Nature, V. 168

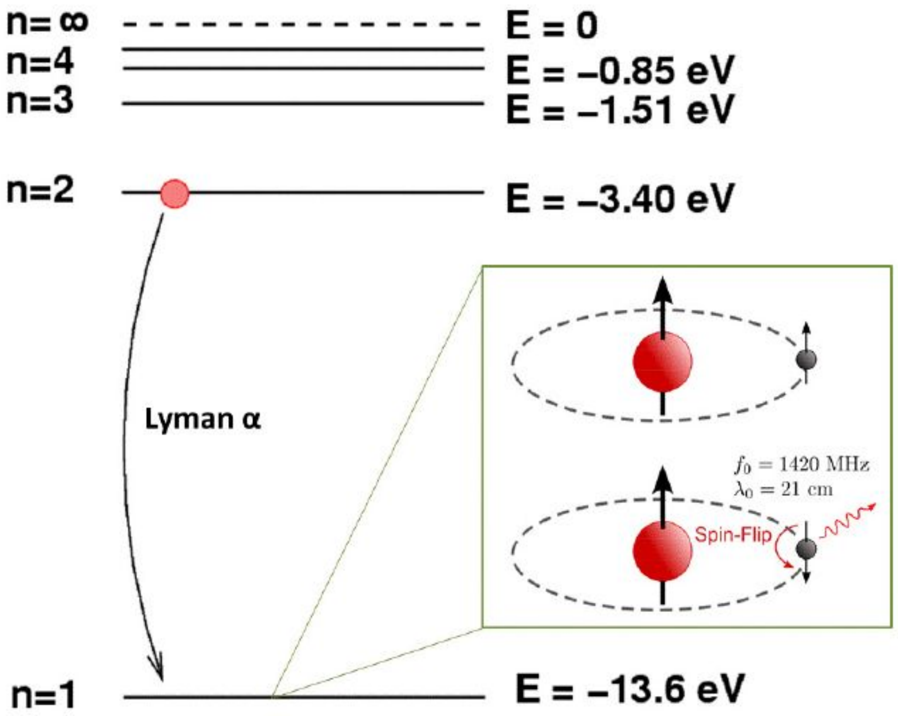

https://arxiv.org/pdf/1605.04357.pdf

Oort et al. https://doi.org/10.1093/mnras/118.4.379

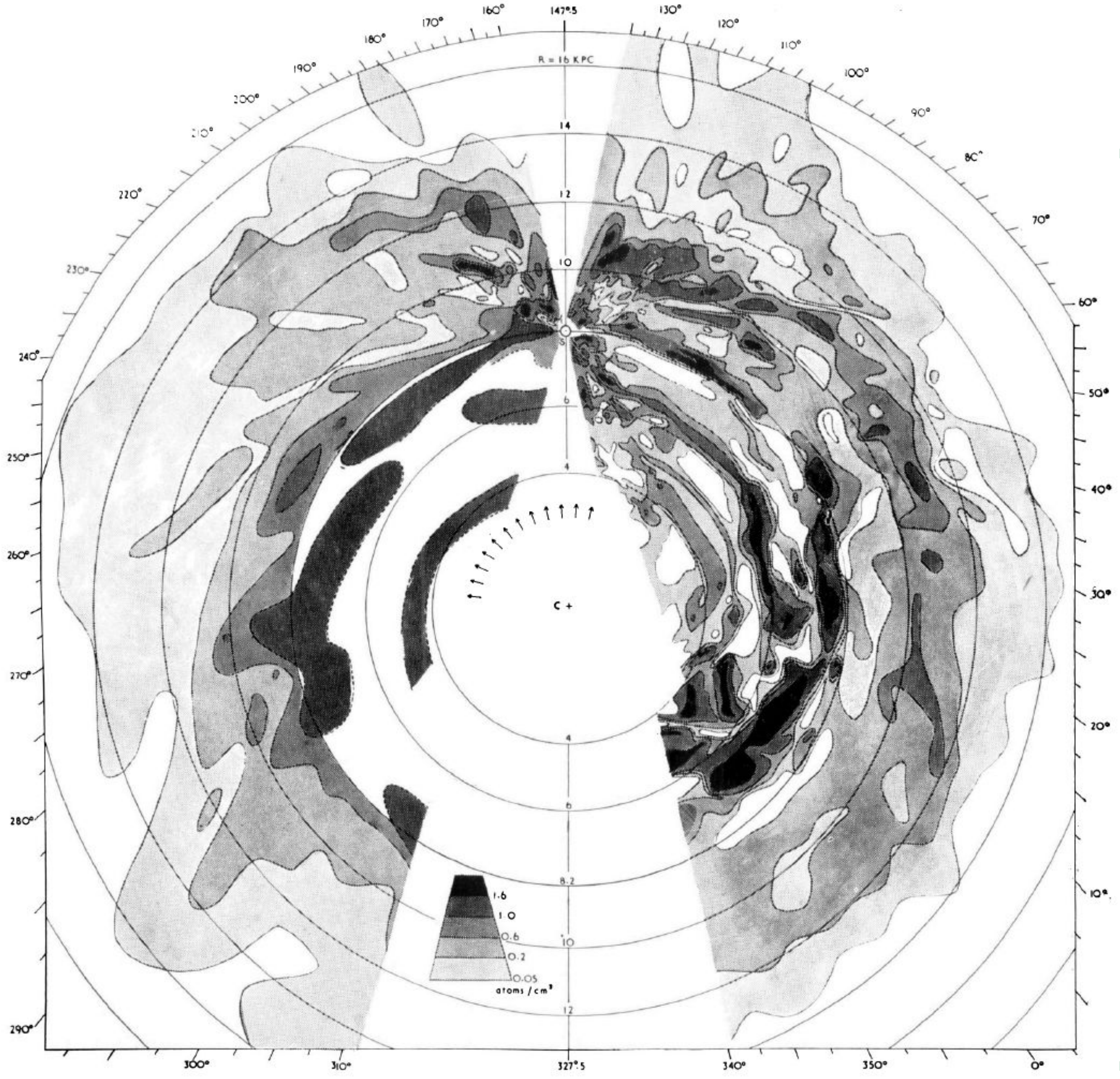

FIG. 4.—*Distribution of neutral hydrogen in the Galactic System. The maximum densities in the z-direction are projected on the galactic plane, and contours are drawn through the points.*

This pr
funding
Union's
researc
prograi
agreem

History of radio astronomy: **Andromeda galaxy** 1950+

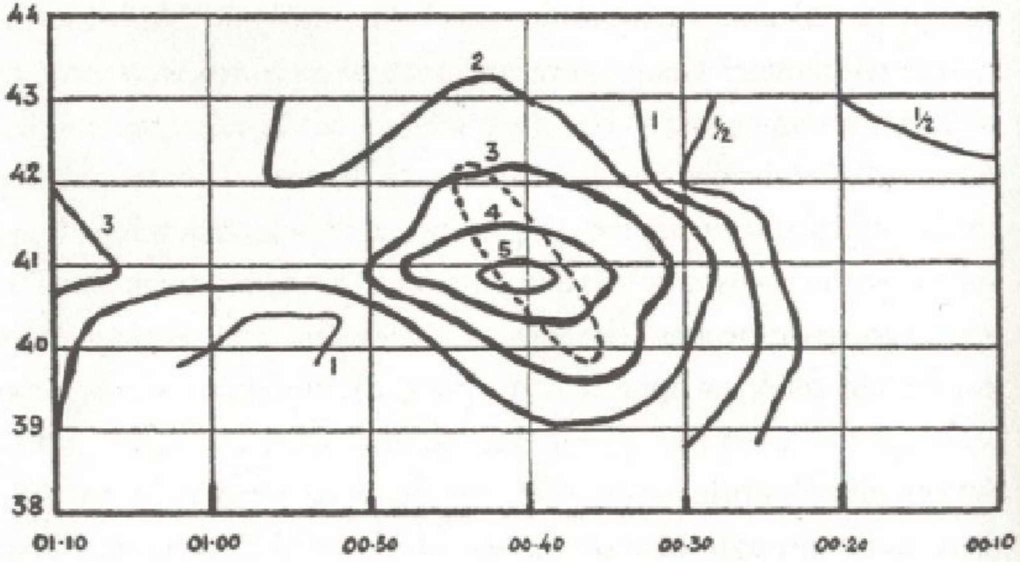

FIGURE 7 The Andromeda Nebula. A radio map made in 1950 with the 218-foot paraboloid radio telescope at Jodrell Bank. *Courtesy of Oxford University Press and the Monthly Notices of the Royal Astronomical Society.*

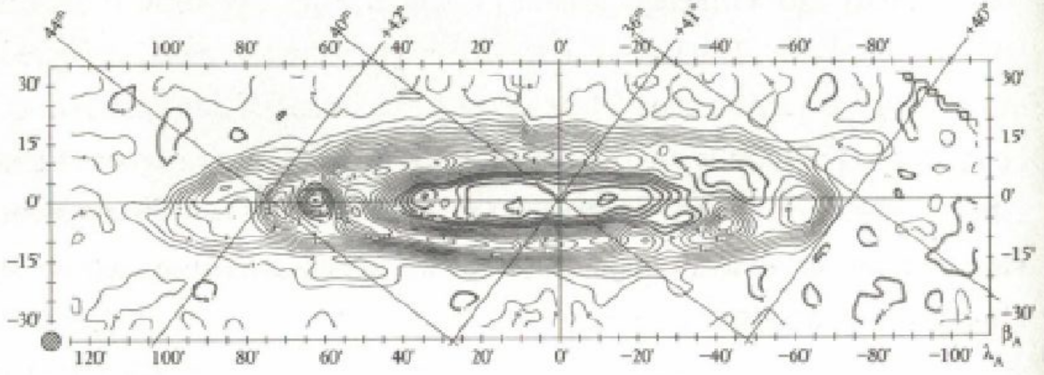

FIGURE 8 A modern radio map of the Andromeda Nebula. A radio map made in 1974 with the 100-metre radio telescope at Effelsberg, Germany. A short wavelength was used, giving the telescope a narrow beam only 5 minutes of arc across. *Berkhuijsen, E. M., Astronomy & Astrophysics, vol 57, page 14, 1977, reproduced with permission © ESO.*

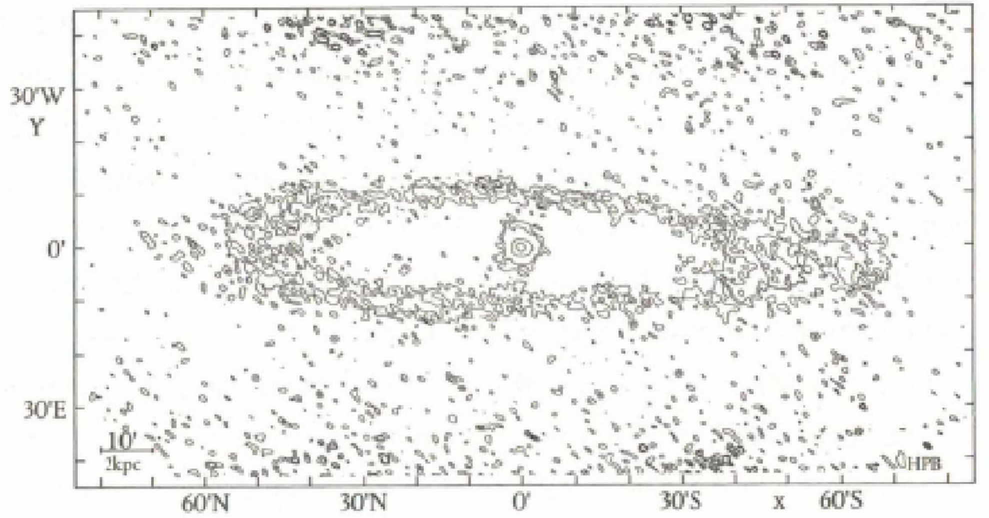

FIGURE 18 Radio map of the Andromeda Nebula, showing a bright source at the centre. An early example of a map made using an aperture synthesis telescope, the WSRT. *Bystedt, J.E.V. et al., Astronomy & Astrophysics, vol 56, page 277, 1984, reproduced with permission © ESO.*

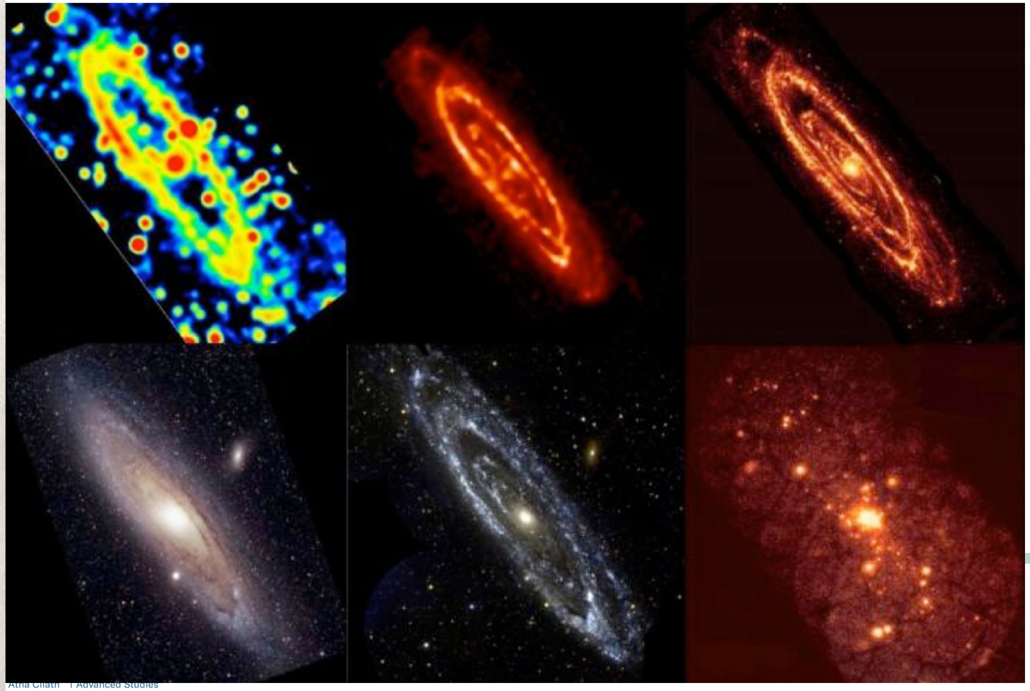

Credit:
Unseen cosmos; https://www.astron.nl/education/what-do-radio-astronomers-see/ (radio, far IR, near-IR, visible, UV, X-ray)

This project has received funding from the European Union's Horizon 2020 research and innovation programme under grant agreement No 952439.

Scientific and Tech
Advan

History of radio astronomy: **Pulsars**

new (2048) antenna field built in UK (1/10 sec) by Antony Hewish & Jocelyn Bell Burnell

1967: first pulsar (PSR B1919+21) discovered by Jocelyn Bell Burnell

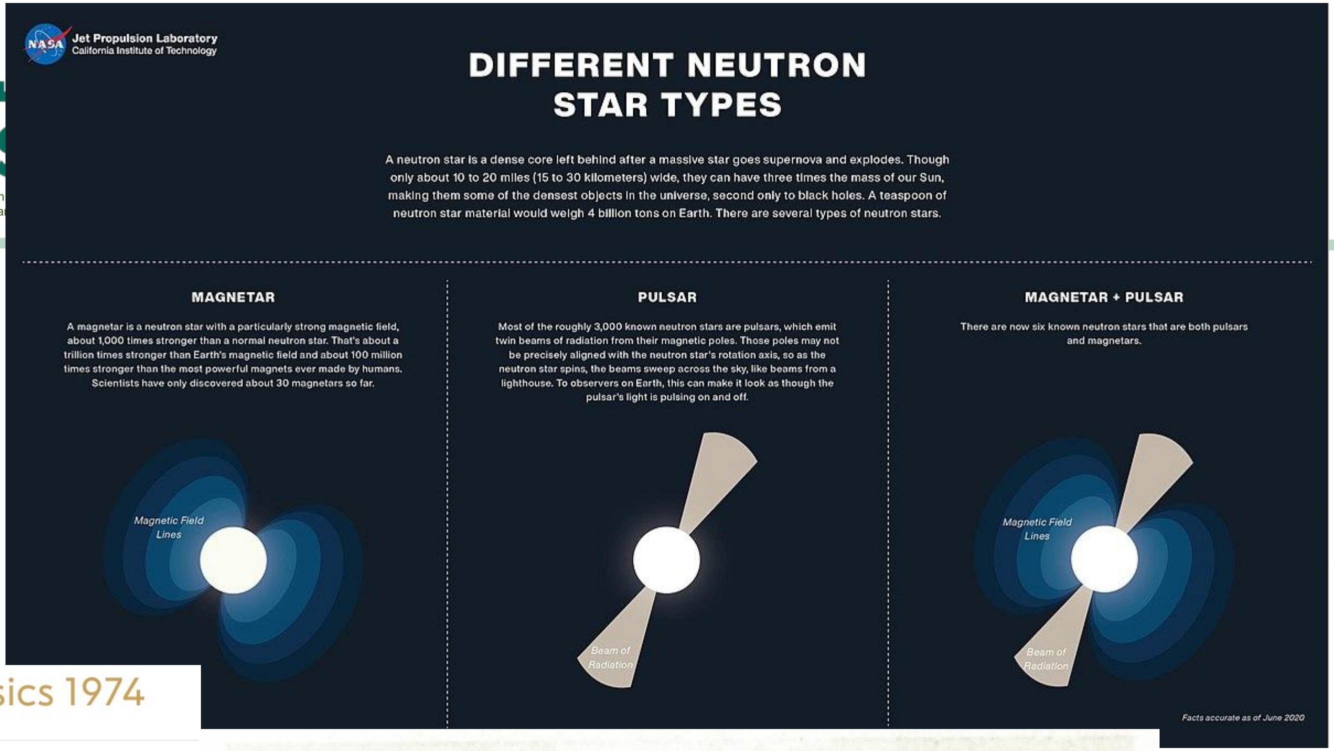

The Nobel Prize in Physics 1974

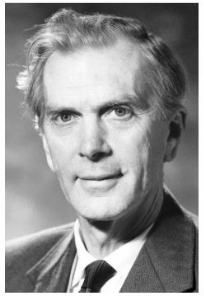

Photo from the Nobel Foundation archive.
Sir Martin Ryle
Prize share: 1/2

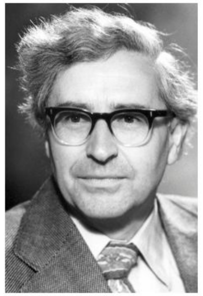

Photo from the Nobel Foundation archive.
Antony Hewish
Prize share: 1/2

The Nobel Prize in Physics 1974 was awarded jointly to Sir Martin Ryle and Antony Hewish "for their pioneering research in radio astrophysics: Ryle for his observations and inventions, in particular of the aperture synthesis technique, and Hewish for his decisive role in the discovery of pulsars"

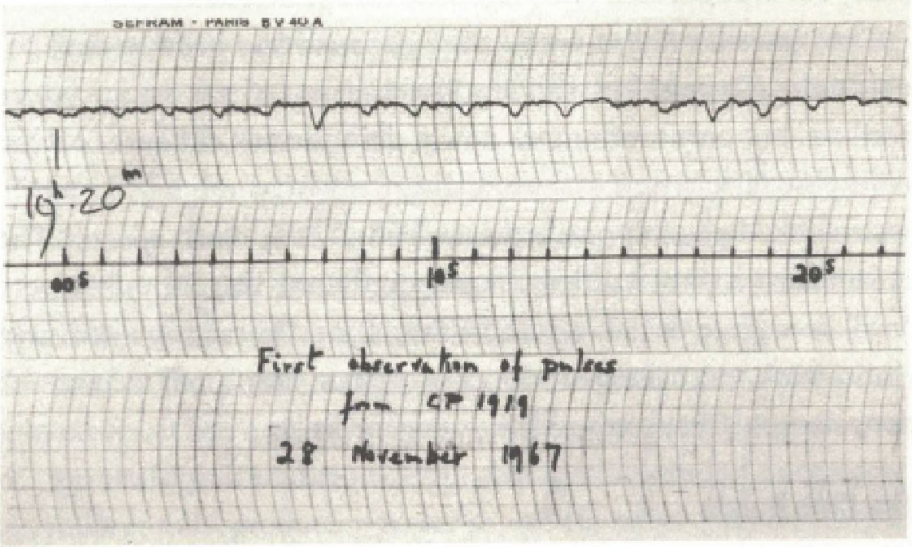

FIGURE 38 The first pulsar recording. The pulses appear at exact intervals of 1.337 seconds.

Credit: Wikipedia; https://www.nobelprize.org/; Unseen cosmos

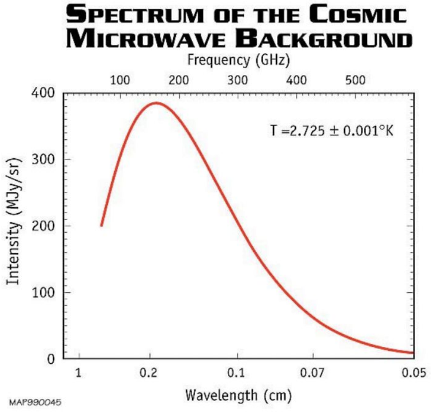

STELLAR

Scientific and Technological Excellence by Leveraging LOFAR Advancements in Radio Astronomy

History of radio astronomy:
cosmic microwave background (CMB) radiation
1964: uniform emission @ ~3 K by Penzias & Wilson

The Nobel Prize in Physics 1978

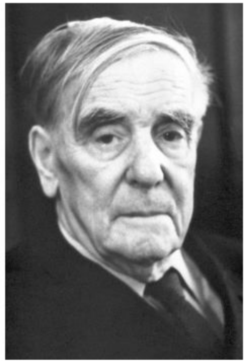

Photo from the Nobel Foundation archive.

Pyotr Leonidovich Kapitsa

Prize share: 1/2

Photo from the Nobel Foundation archive.

Arno Allan Penzias

Prize share: 1/4

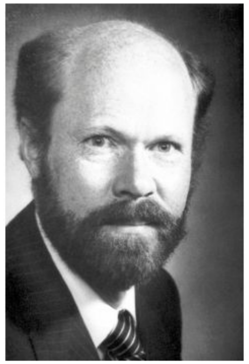

Photo from the Nobel Foundation archive.

Robert Woodrow Wilson

Prize share: 1/4

The Nobel Prize in Physics 1978 was divided, one half awarded to Pyotr Leonidovich Kapitsa "for his basic inventions and discoveries in the area of low-temperature physics", the other half jointly to Arno Allan Penzias and Robert Woodrow Wilson "for their discovery of cosmic microwave background radiation"

https://www.nobelprize.org/

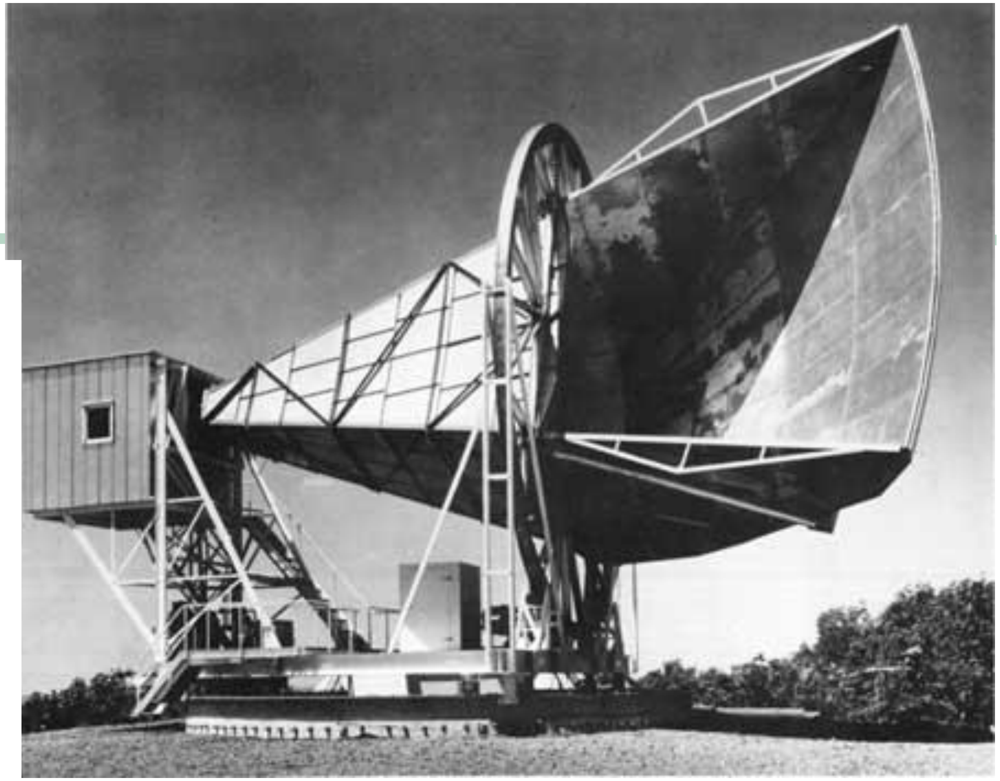

https://www.cv.nrao.edu/~sransom/web/Ch3.html#S6

A summary of measurements of the CMB temperature T_R

Frequency (GHz)	T_R	Ref.
0.408–0.610	3.7±1.2	Howell & Shakeshaft (1967)
0.6	3.0±1.2	Sironi et al. (1990)
0.82	2.7±1.6	Sironi et al. (1991)
1.4	2.65±0.33	Staggs et al. (1996a)
2.0	2.55±0.14	Bersanelli et al. (1995)
2.5	2.79±0.15	Sironi & Bonelli (1986)
10.7	2.730±0.014	Staggs et al. (1996b)
25	2.783±0.025	Johnson & Wilkinson (1987)
60–600	2.725±0.002	Mather et al. (1999)

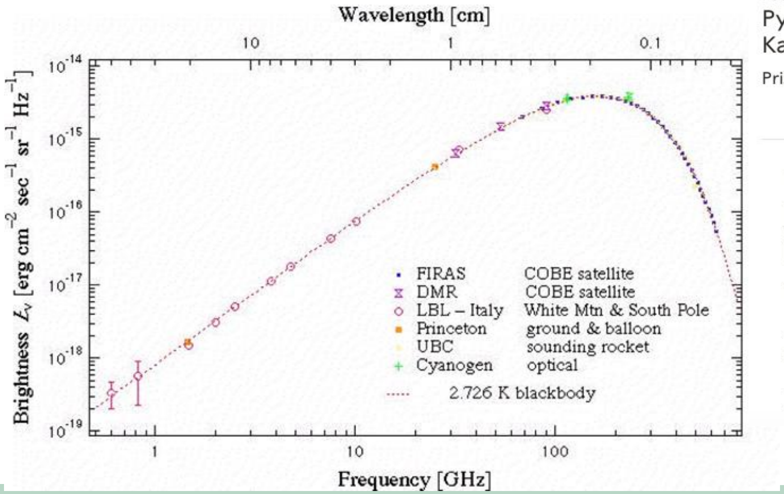

https://ned.ipac.caltech.edu/level5/Sept05/Gawiser2/Gawiser2.html

ASTRON

DIAS

Institiúid Ard-Léinn Bhaile Átha Cliath | Dublin Institute for Advanced Studies

https://doi.org/10.1016/S1387-6473(99)00016-0

This project has received funding from the European Union's Horizon 2020 research and innovation programme under grant agreement No 952439.

STELLAR
Scientific and Technological Excellence by Leveraging LOFAR Advancements in Radio Astronomy

Institute of Astronomy – National Astronomical Observatory

History of radio astronomy:
Binary pulsars & indirect proof for gravitational waves

Arecibo observations/1974

declining orbit period of the system/1978

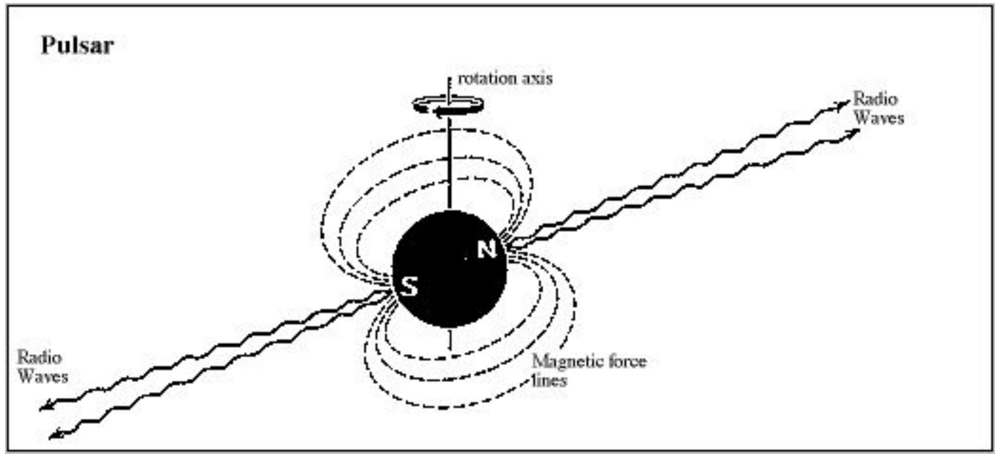

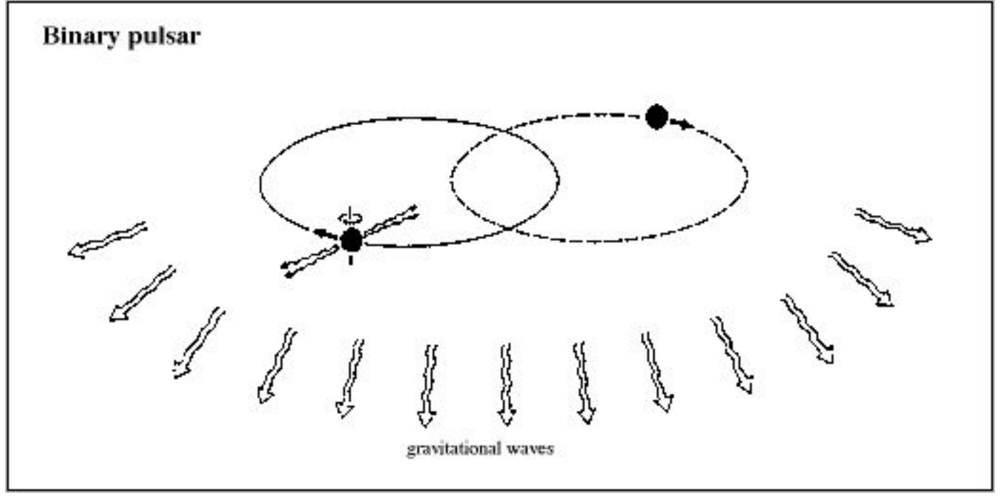

The Nobel Prize in Physics 1993


Photo from the Nobel Foundation archive.
Russell A. Hulse
Prize share: 1/2


Photo from the Nobel Foundation archive.
Joseph H. Taylor Jr.
Prize share: 1/2

The Nobel Prize in Physics 1993 was awarded jointly to Russell A. Hulse and Joseph H. Taylor Jr. "for the discovery of a new type of pulsar, a discovery that has opened up new possibilities for the study of gravitation"

https://www.nobelprize.org/

ASTRON DIAS
Institiúid Ard-Léinn Bhaile Átha Cliath | Dublin Institute for Advanced Studies

This project has received funding from the European Union's Horizon 2020 research and innovation programme under grant agreement No 952439.

STELLA
Scientific and Technological Excellence by Leveraging LO[FAR] Advancements in Radio Astronomy

Recent discoveries:
Protoplanetary disks

https://www.eso.org/public/images/potw1904a/

2019

ALMA

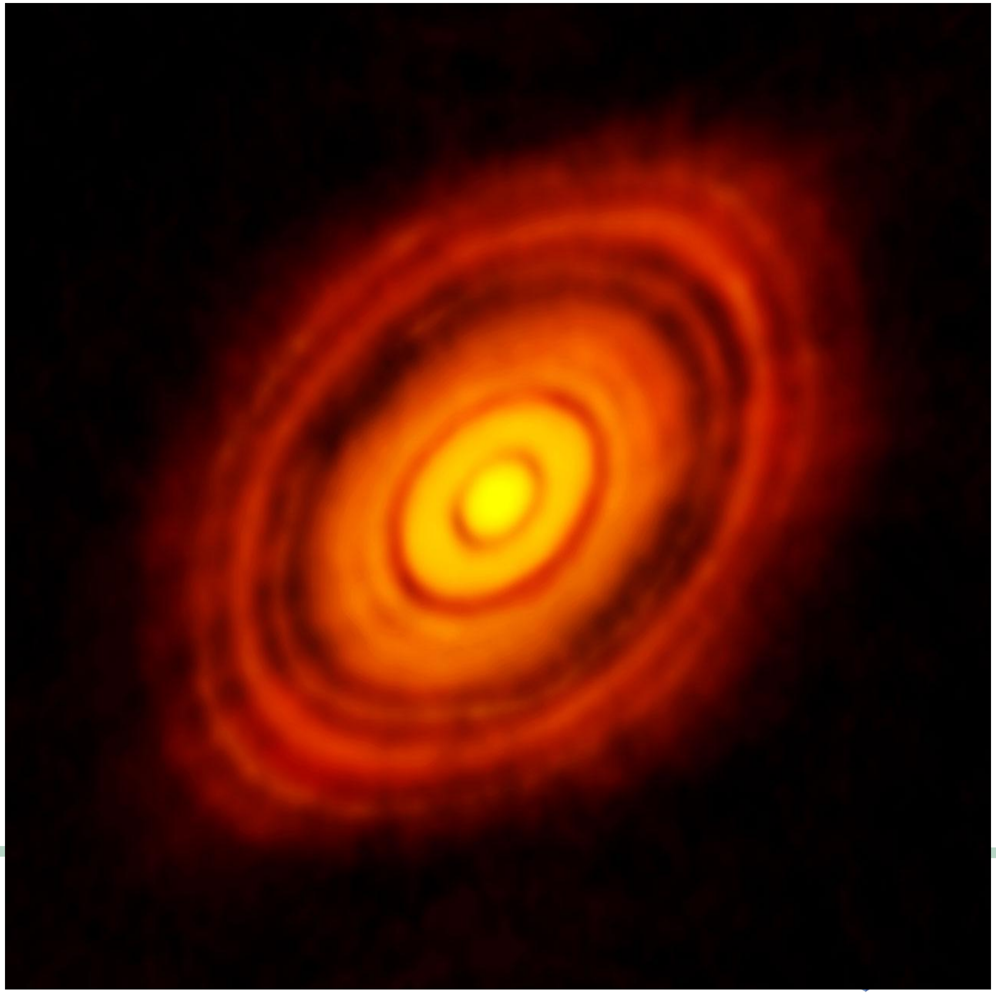

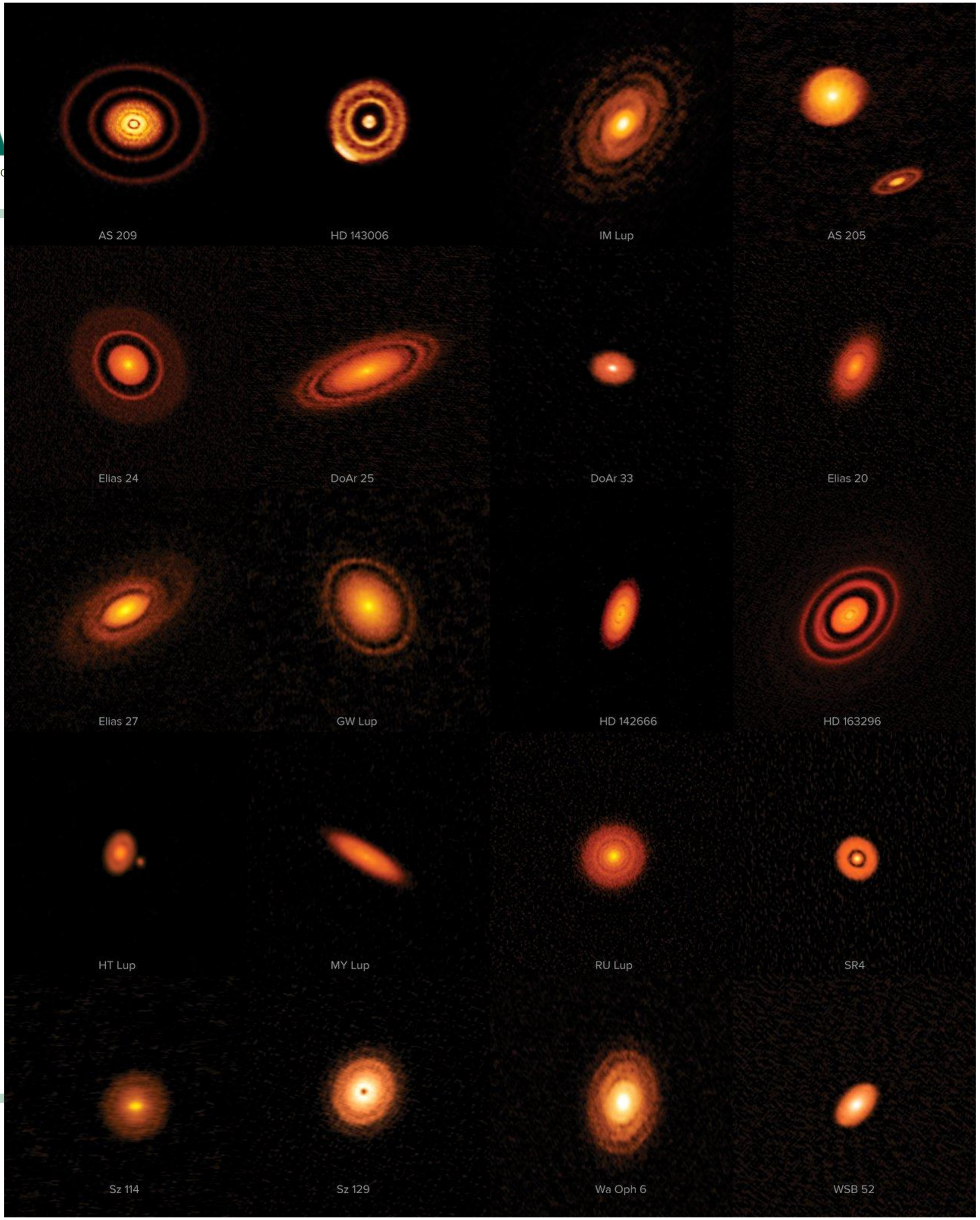

This project has received funding from the European Union's Horizon 2020 research and innovation programme under grant agreement No 952439.

STELLAR
Scientific and Technological Excellence by Leveraging LOFAR Advancements in Radio Astronomy

INSTITUTE OF ASTRONOMY
NATIONAL ASTRONOMICAL OBSERVATORY

Recent discoveries:
M87 BH

10 April 2019

Event Horizon Telescope (EHT) Collaboration

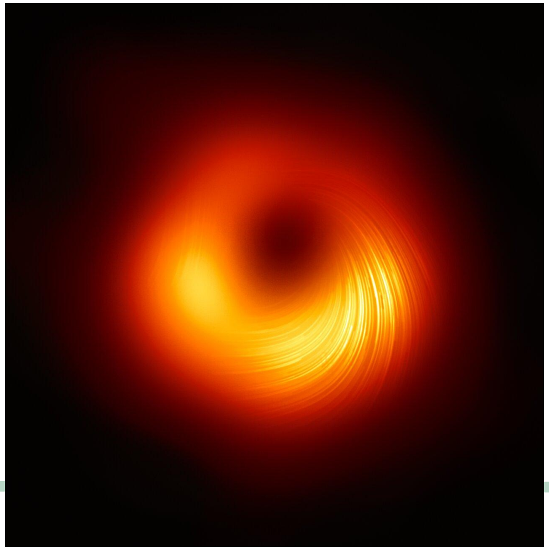

https://www.eso.org/public/images/eso2105a/

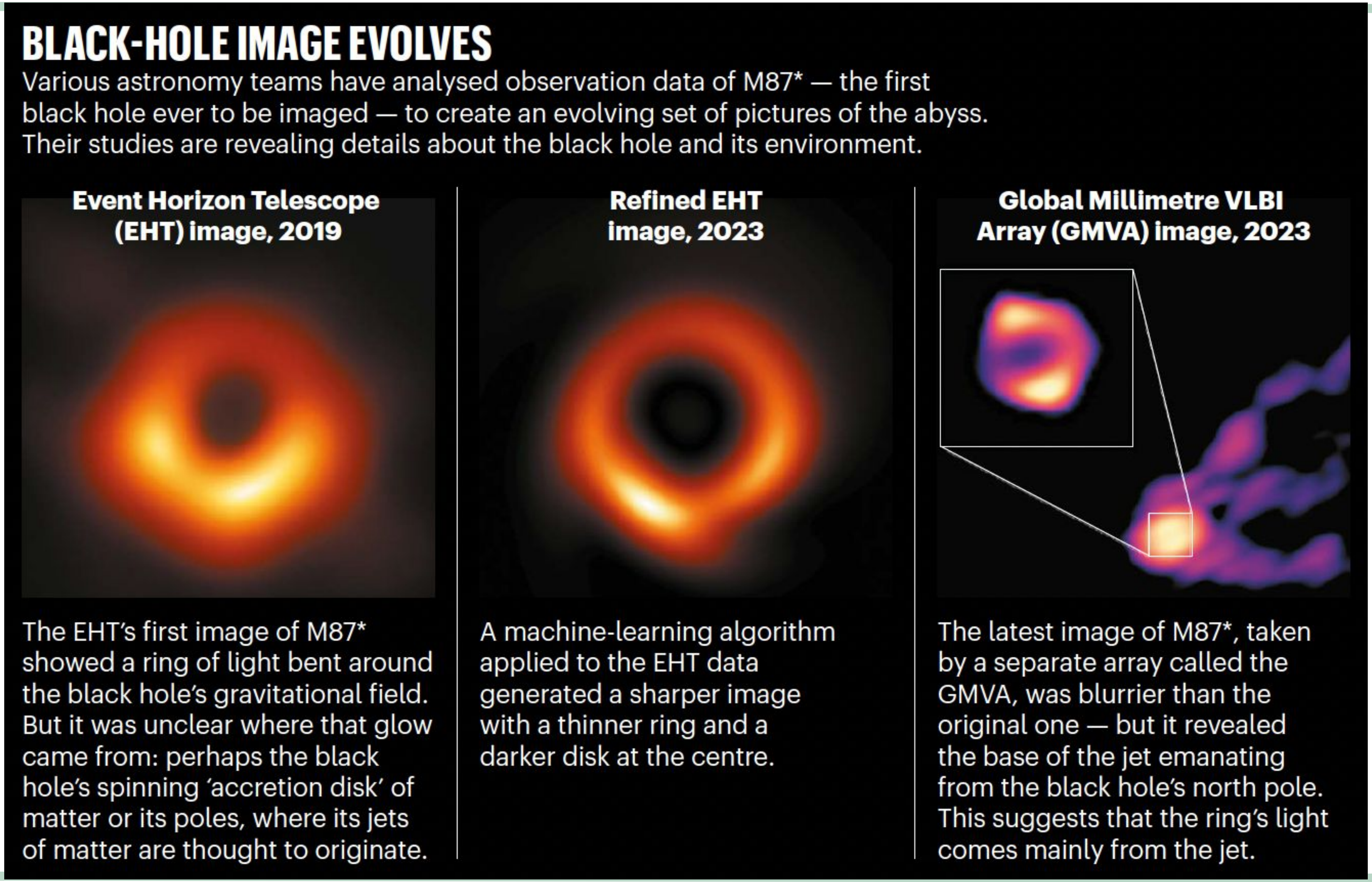

ASTRON

DIAS
Institiúid Ard-Léinn Bhaile Átha Cliath | Dublin Institute for Advanced Studies

https://www.nature.com/articles/d41586-023-01442-x

This project has received funding from the European Union's Horizon 2020 research and innovation programme under grant agreement No 952439.

STELLAR
Scientific and Technological Excellence by Leveraging LOFAR Advancements in Radio Astronomy

Recent discoveries:
Milky way BH/Sgr A

12 May 2022

Event Horizon Telescope (EHT) Collaboration

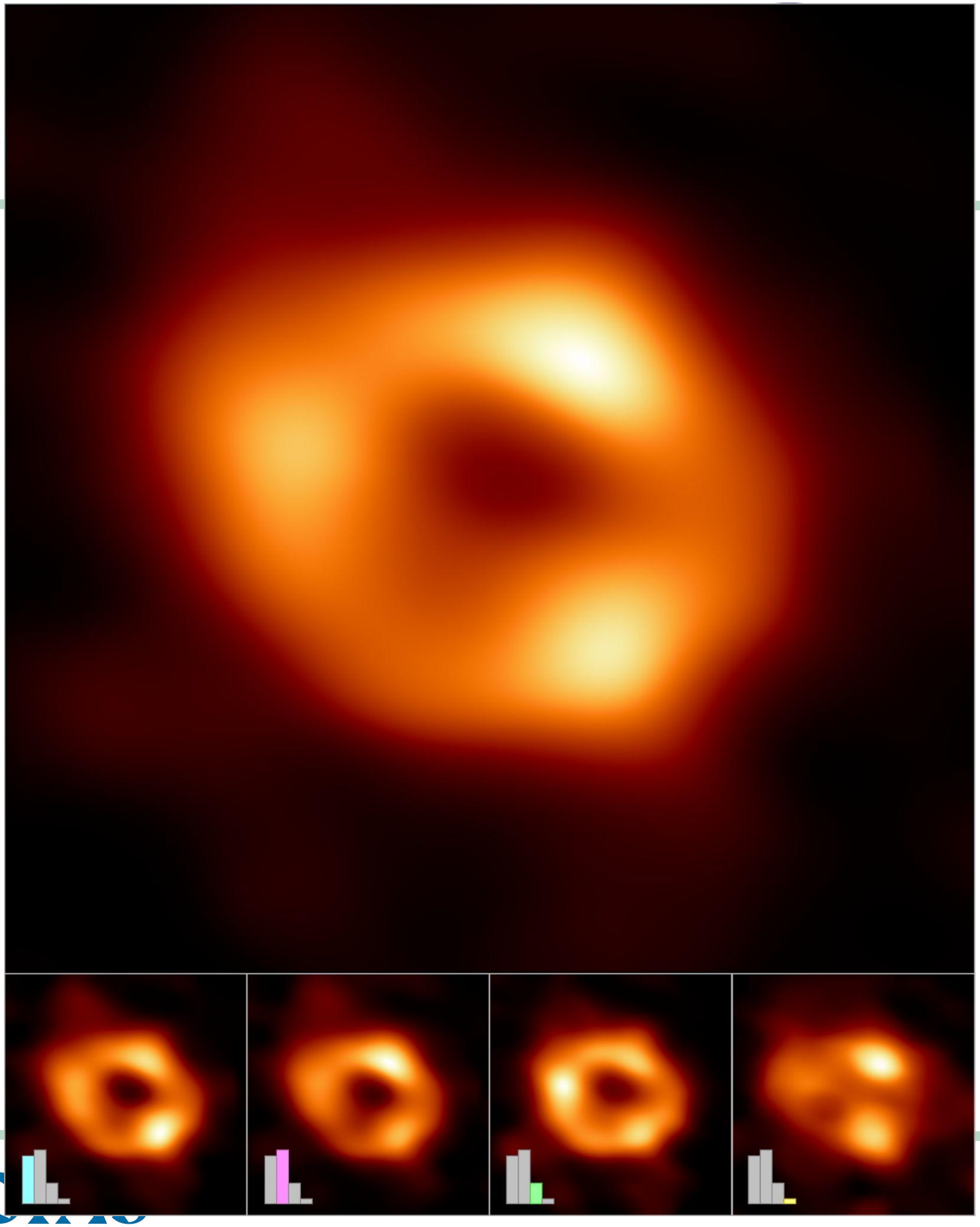

https://eventhorizontelescope.org/
https://cdn.eso.org/images/large/eso2208-eht-mwb.jpg

ASTRON

Institiúid Ard-Léinn Bhaile Átha Cliath | Dublin Institute for Advanced Studies

This project has received funding from the European Union's Horizon 2020 research and innovation programme under grant agreement No 952439.

STELLAR
Scientific and Technological Excellence by Leveraging LOFAR Advancements in Radio Astronomy

INSTITUTE OF ASTRONOMY NATIONAL ASTRONOMICAL OBSERVATORY

Emission mechanisms in radio domain

I. Distribution function

Thermal: Blackbody radiation

Nonthermal: Free-free; Coherent

II. Emission

Incoherent: emission from individual electrons (free-free; gyro)

Coherent: emission from the entire distribution (plasma; maser)

III. Spectrum

Continuum source: source emitting over a broad frequency range

Spectral-line source: source emitting at narrow lines, at specific frequencies

IV. Location

Galactic source

Extragalactic source

ASTRON

DIAS
Institiúid Ard-Léinn | Dublin Institute for
Bhaile Átha Cliath | Advanced Studies

This project has received funding from the European Union's Horizon 2020 research and innovation programme under grant agreement No 952439.

STELLAR
Scientific and Technological Excellence Advancements in Radio A

https://www.radio2space.com/category/radio-astronomy-projects/

I.

Thermal emission
(Blackbody radiation/Planck-law)
- HII regions
- planetary nebulae
- weak solar flares

vs.

Non-thermal emission
(power-law)
- AGN, quasars
- Jupiter magnetosphere
- star formation regions
- strong solar flares

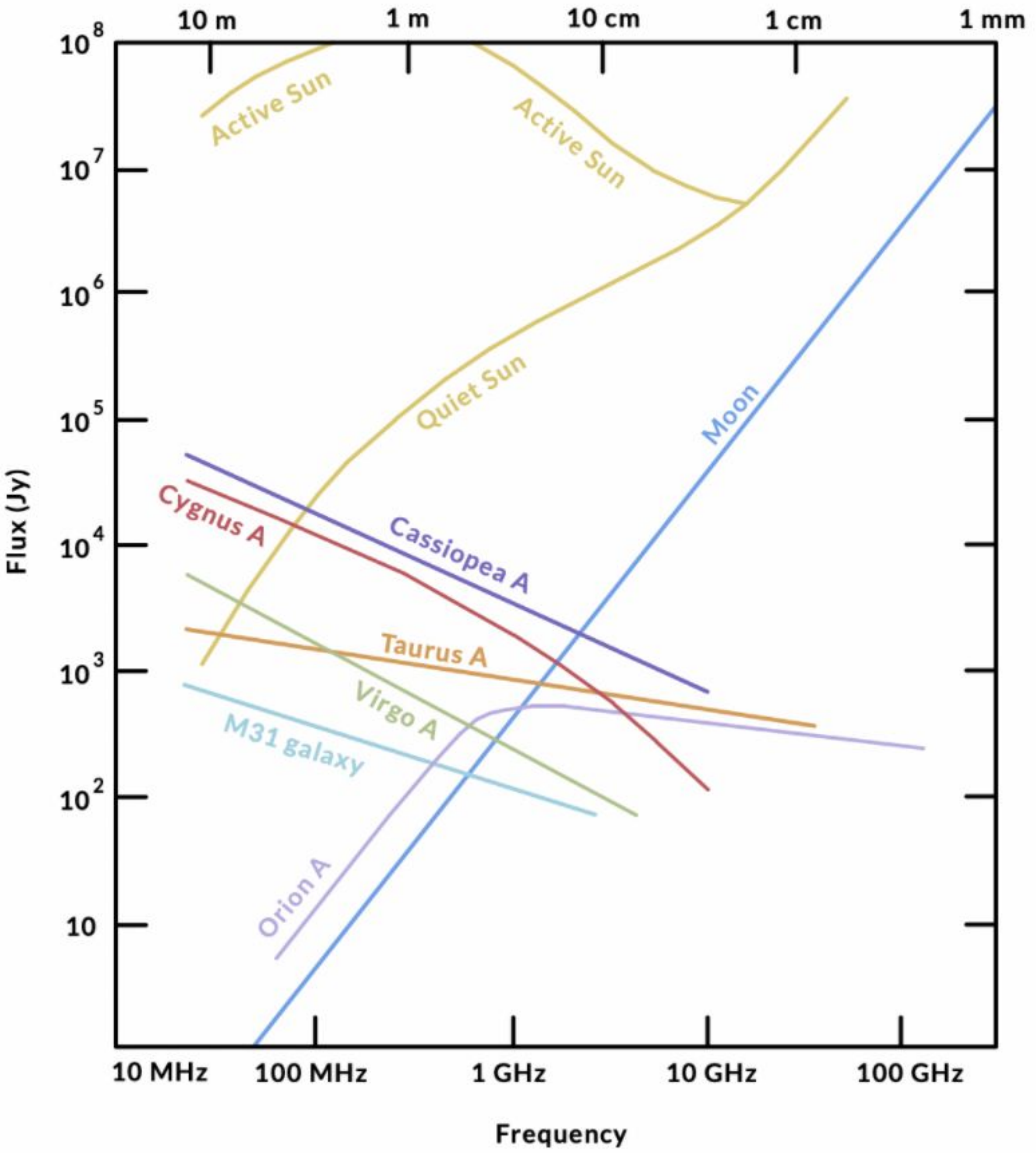

ASTRON

This project has received funding from the European Union's Horizon 2020 research and innovation programme under grant agreement No 952439.

STELLAR

Scientific and Technological Excellence by Leveraging LOFAR Advancements in Radio Astronomy

INSTITUTE OF ASTRONOMY NATIONAL ASTRONOMICAL OBSERVATORY

Blackbody radiation

(McKean, 2022)

- The spectral brightness B_ν at frequency ν of a blackbody object (stars) is given by Planck's law.

Spectral brightness (W m^{-2} Hz^{-1} sr^{-1})

Planck constant = 6.626 x 10^{-34} m^2 kg s^{-1}

$$B_\nu(T) = \frac{2h\nu^3}{c^2}\frac{1}{\exp\frac{h\nu}{kT} - 1}$$

Speed of light constant = 3 x 10^8 m s^{-1}

Absolute temperature (K)

- In the low frequency radio limit, $h\nu / kT \ll 1$.

$$B_\nu(T) \approx \frac{2h\nu^3}{c^2}\frac{kT}{h\nu} = \frac{2kT\nu^2}{c^2} = \frac{2kT}{\lambda^2}$$

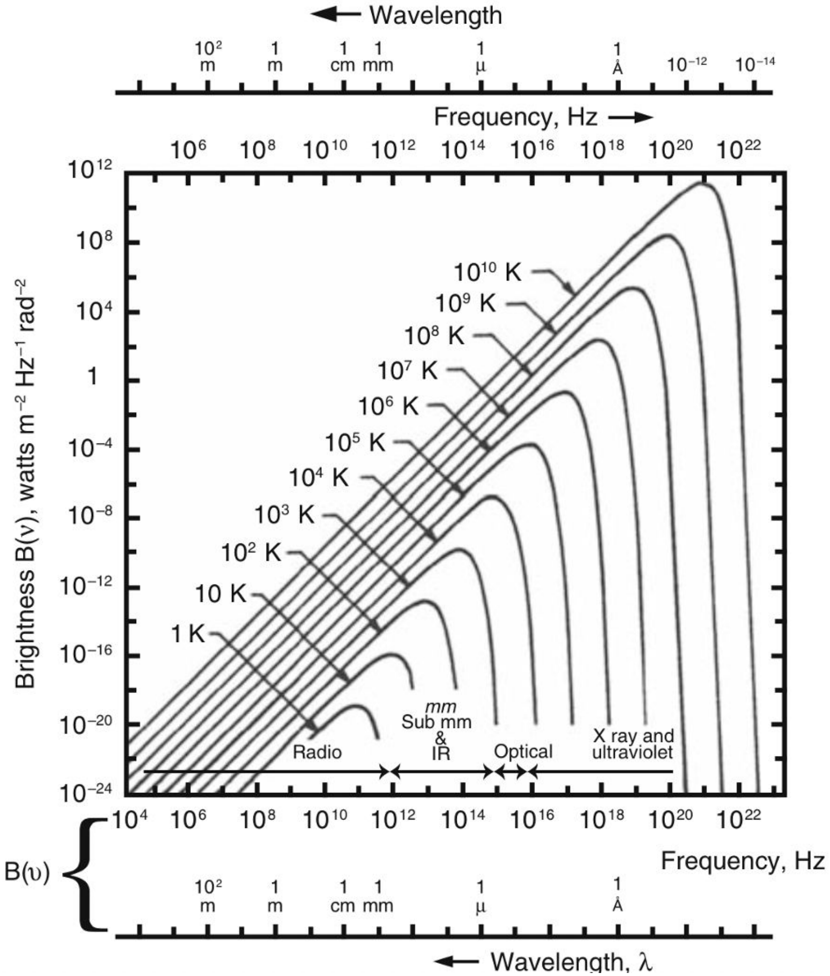

ASTRON

DIAS

Institiúid Ard-Léinn Bhaile Átha Cliath | Dublin Institute for Advanced Studies

This project has received funding from the European Union's Horizon 2020 research and innovation programme under grant agreement No 952439.

II.

Incoherent
vs.
Coherent

Table 15.1: Radio emission mechanisms during solar flares, (gyrofrequences are given in units of angular frequencies, $\omega = 2\pi\nu$) (Aschwanden 2002b).

Emission mechanism	Frequency	Source/Exciter
(1) Incoherent radio emission:		
(1a) Free-free emission (bremsstrahlung)	$\nu \gtrsim 1$ GHz	Thermal plasma
– Microwave postbursts		Thermal plasma
(1b) Gyroemission	$\omega = s\Omega_e$	
Gyroresonance emission	$(s = 1, 2, 3, 4)$	Thermal electrons
Gyrosynchrotron emission	$(s \approx 10 - 100)$	Mildly relativistic electrons
– Type IV moving		Trapped electrons
– Microwave type IV		Trapped electrons
(2) Coherent radio emission:		
(2a) Plasma emission	$\nu_{pe} = 9000\sqrt{n_e}$	Electron beams
– Type I storms		Langmuir turbulence
– Type II bursts		Beams from shocks
– Type III bursts		Upward propagating beams
– Reverse slope (RS) bursts		Downward propagating beams
– Type J bursts		Beams along closed loops
– Type U bursts		Beams along closed loops
– Type IV continuum		Trapped electrons
– Type V		Slow electron beams
(2b) Electron-cyclotron maser:	$\omega = s\Omega_e/\gamma + k_{\|} v_{\|}$	Losscones
- Decimetric ms spike bursts		Losscones

This project has received funding from the European Union's Horizon 2020 research and innovation programme under grant agreement No 952439.

Incoherent

1. Bremsstrahlung/braking radiation (from plasma - free-free emission/Couloumb collisions)

- electron is free before and after emission
- emission due to electron deceleration in the ion field

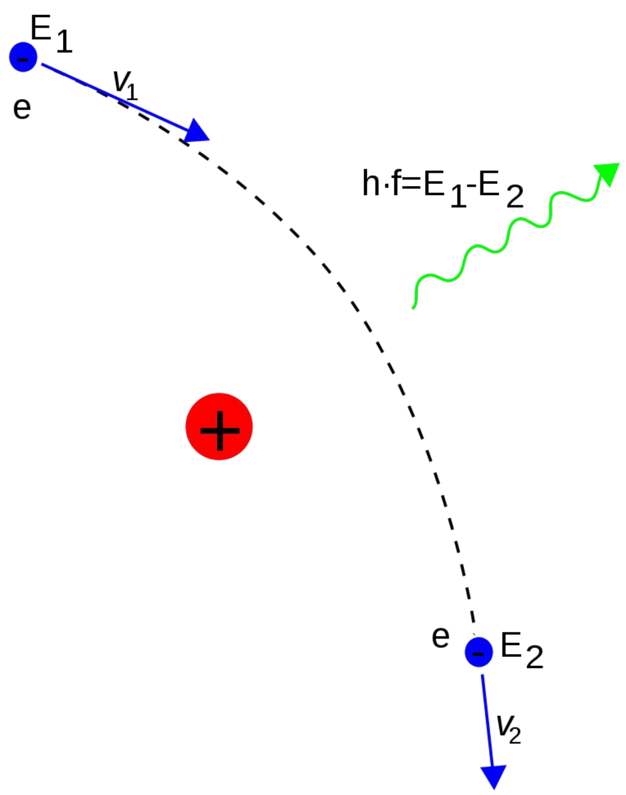

https://en.wikipedia.org/wiki/Bremsstrahlung

This project has received funding from the European Union's Horizon 2020 research and innovation programme under grant agreement No 952439.

STELLAR
Scientific and Technological Excellence by Leveraging LOFAR Advancements in Radio Astronomy

Incoherent

2. Cyclotron (gyro-synchrotron): non-relativistic case/thermal electrons

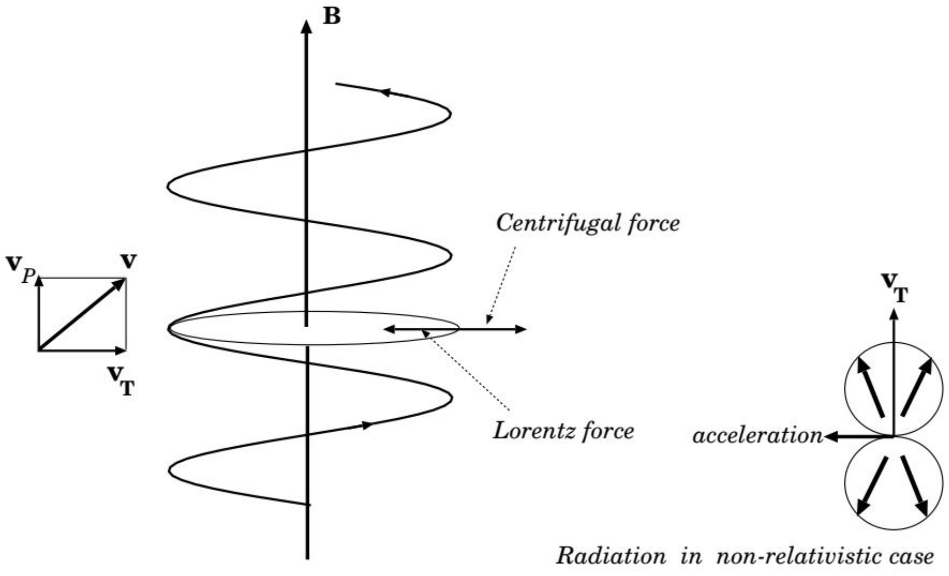

Figure 28: "Cyclotron" or "Gyro–synchrotron" radiation

3. Synchrotron: relativistic electrons

- extremely intense and highly collimated radiation: the radiation seems to be coming from a thin cone
- emitted over a wide range of energies, producing a wide energy spectrum
- highly polarised, with the degree and orientation of the polarisation providing information about the magnetic fields of the source

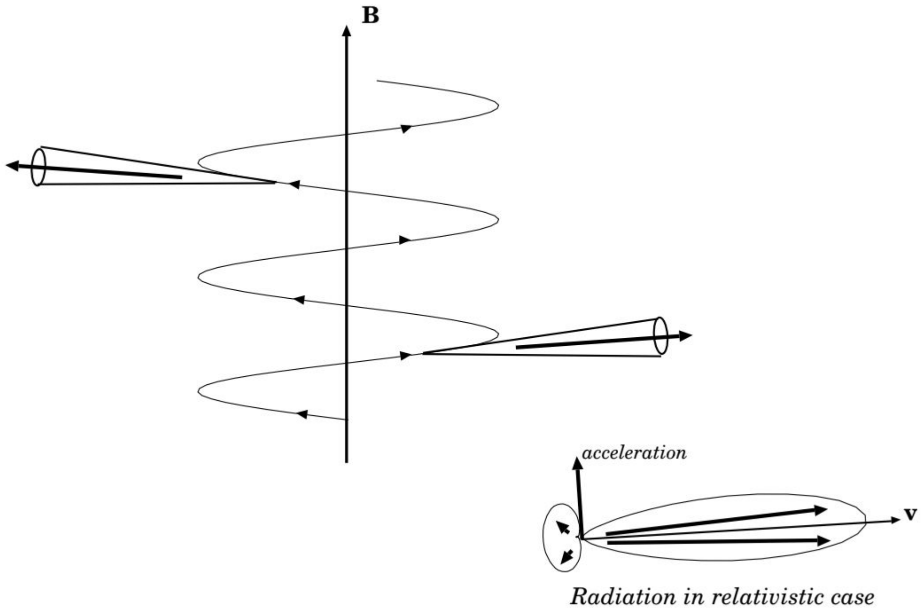

Figure 29: Synchrotron radiation from a relativistic electron.

image credit: Tetsuo Sasao and Andre B. Fletcher, Lecture notes, 2006

This project has received funding from the European Union's Horizon 2020 research and innovation programme under grant agreement No 952439.

STELLAR
Scientific and Technological Excellence by Leveraging LOFAR Advancements in Radio Astronomy

INSTITUTE OF ASTRONOMY NATIONAL ASTRONOMICAL OBSERVATORY

Coherent
Plasma emission

Reid and Ratcliffe, 2014

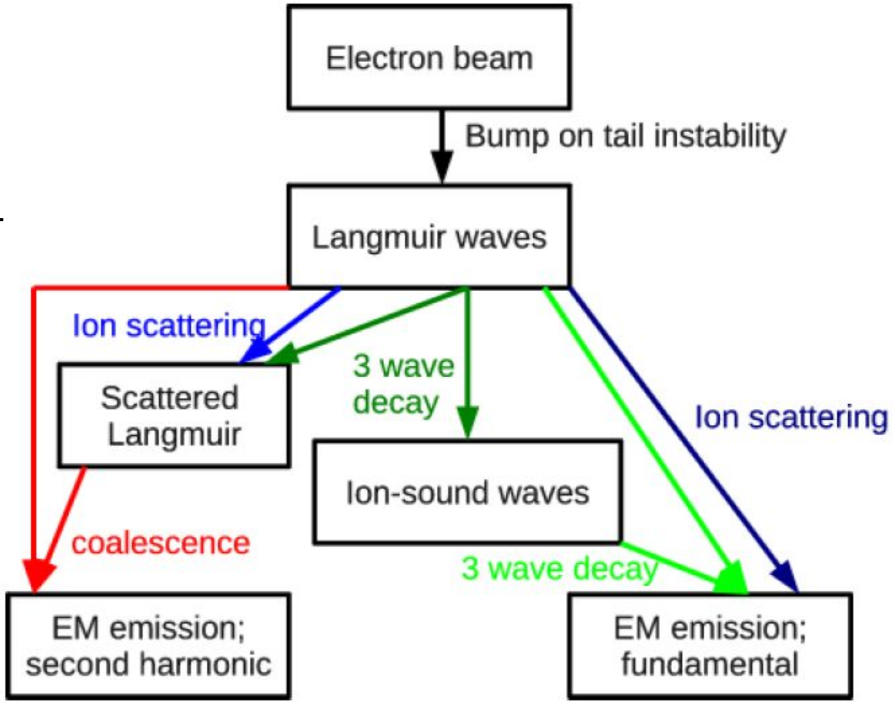

Fig. 2 A flow diagram indicating the stages in plasma emission in an updated version on the original theory (adapted from Melrose 2009).

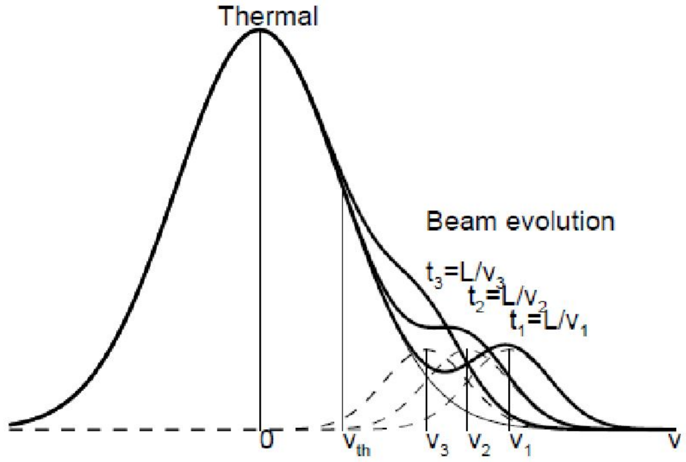

Figure 15.10: The evolution of a beam in the tail of a thermal distribution is shown, starting with the arrival of the fastest electrons at time $t_1 = L/v_1$, producing a positive slope $\partial f/\partial v > 0$ and which is unstable. At later times, slower electrons arrive at $t_2 = L/v_2$ and $t_3 = L/v_3$, but the slowest ones do not produce a positive slope and are stable (adapted from Lin et al. 1981b).

ASTRON DIAS Institiúid Ard-Léinn Bhaile Átha Cliath | Dublin Institute for Advanced Studies

This project has received funding from the European Union's Horizon 2020 research and innovation programme under grant agreement No 952439.

STELLAR
Scientific and Technological Excellence by Leveraging LOFAR Advancements in Radio Astronomy

INSTITUTE OF ASTRONOMY · NATIONAL ASTRONOMICAL OBSERVATORY

Radio astronomy: studies the cosmic objects via their radio emission (photometry - intensity, spectra - vs. frequency and polarization)

Radio emitting objects
- stars/Sun/pulsars
- planets
- galaxies/active galaxy nuclei/ quasars
- black holes
- ISM/hydrogen clouds

Credit: Zarca & Tagger (2006); Mimoun et al. (2011)

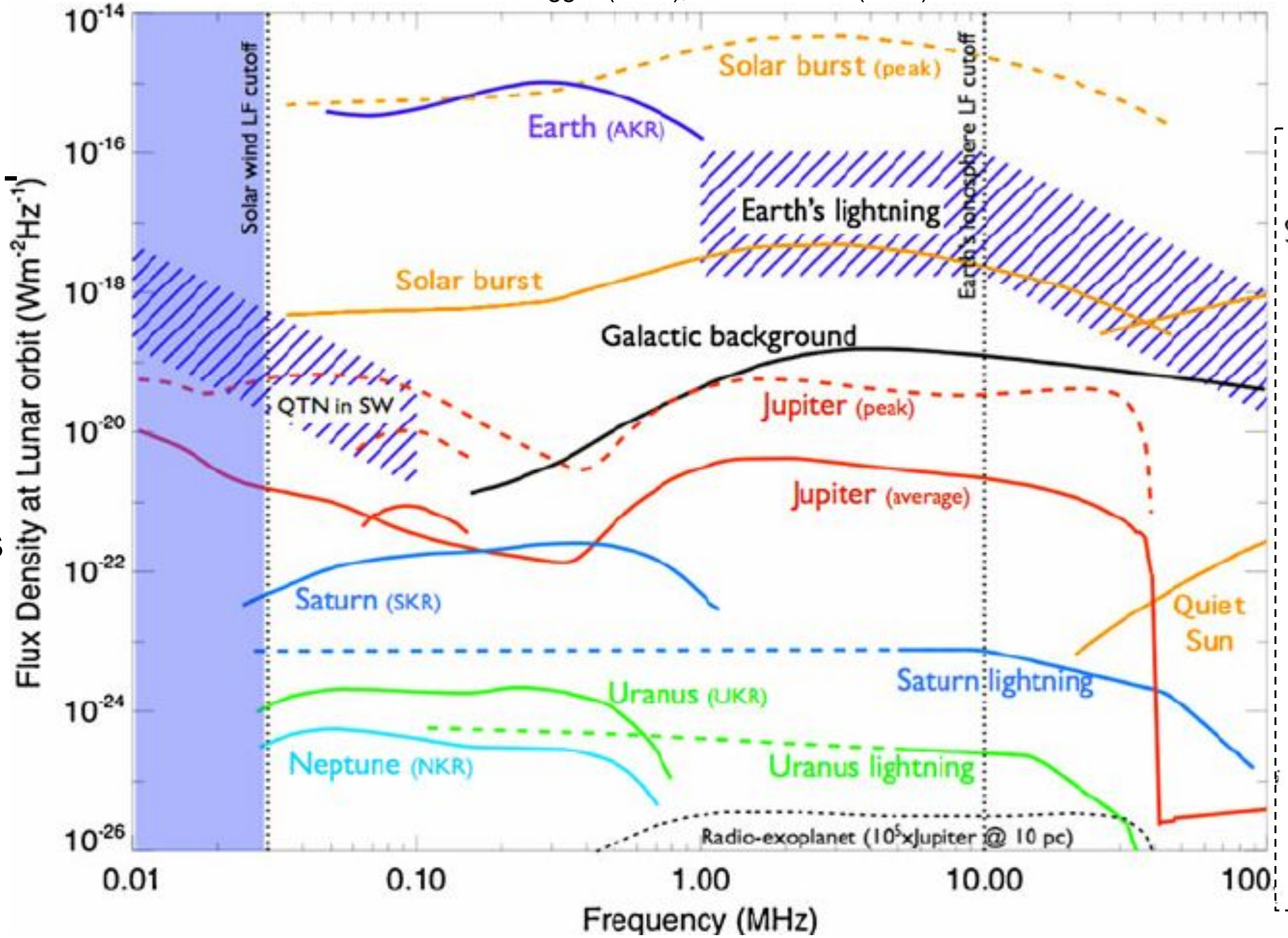

https://www.cv.nrao.edu/~sransom/web/xxx.html

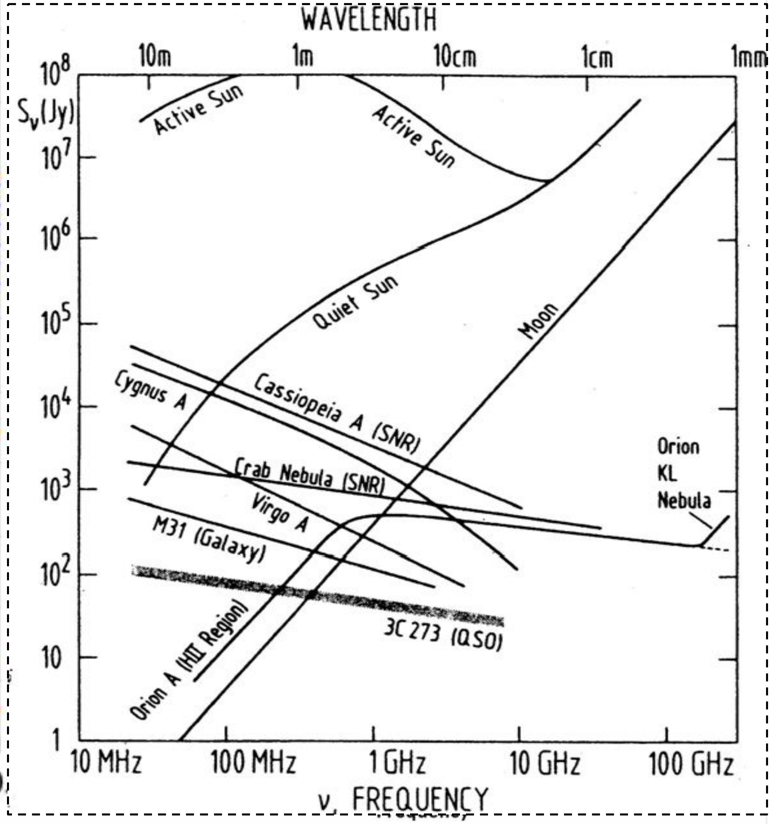

ASTRON

DIAS
Institiúid Ard-Léinn Bhaile Átha Cliath | Dublin Institute for Advanced Studies

This project has received funding from the European Union's Horizon 2020 research and innovation programme under grant agreement No 952439.

STELLAR
Scientific and Technological Excellence by Leveraging LOFAR Advancements in Radio Astronomy

INSTITUTE OF ASTRONOMY
NATIONAL ASTRONOMICAL OBSERVATORY

Composite spectrum of galaxy

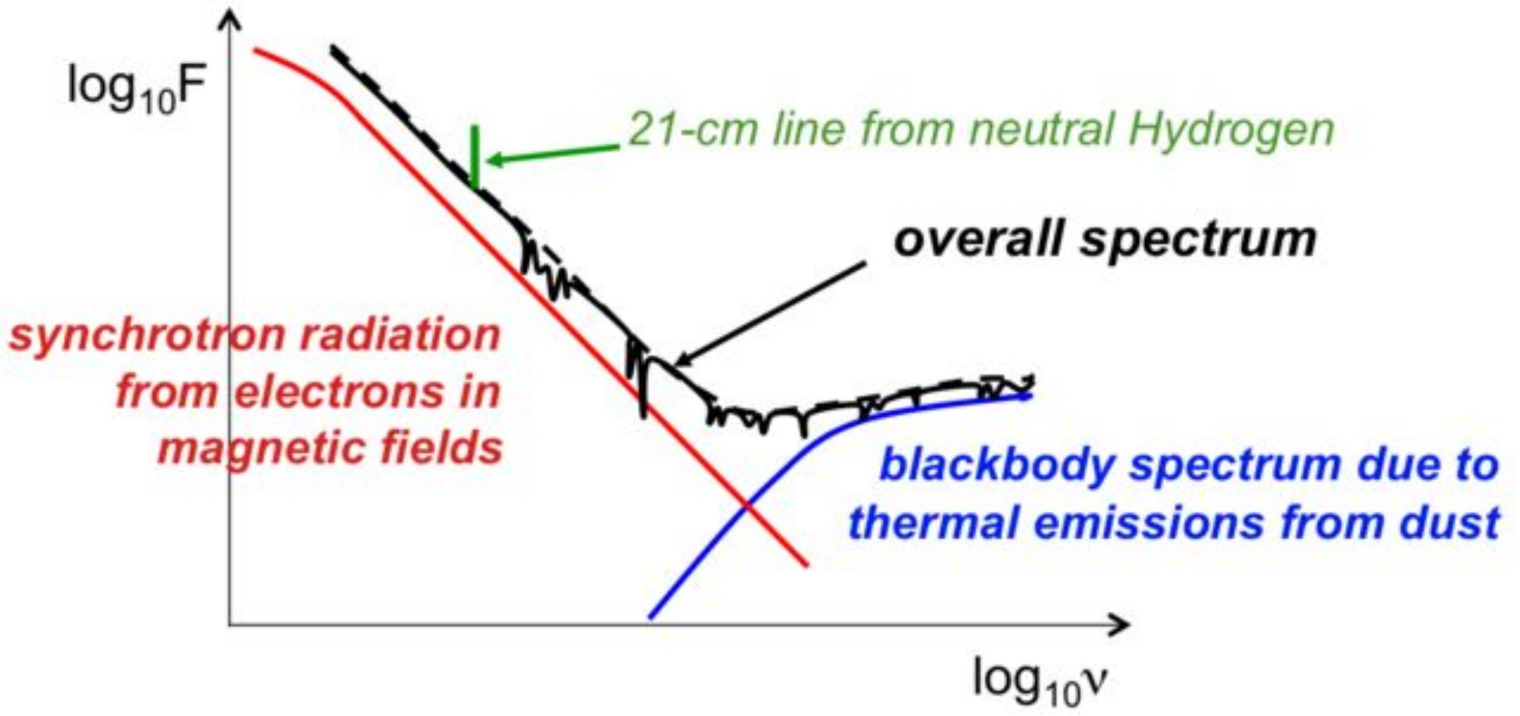

typical extra-galactic source with power-law behaviour: S(ν) ∝ ν^α with spectral index α = –0.7

Credit: Lecture notes from Swinburne University of Technology, 2010

ASTRON

DIAS
Institiúid Ard-Léinn Bhaile Átha Cliath | Dublin Institute for Advanced Studies

This project has received funding from the European Union's Horizon 2020 research and innovation programme under grant agreement No 952439.

STELLAR
Scientific and Technological Excellence by Leveraging LOFAR Advancements in Radio Astronomy

INSTITUTE OF ASTRONOMY
NATIONAL ASTRONOMICAL OBSERVATORY

Real spectra

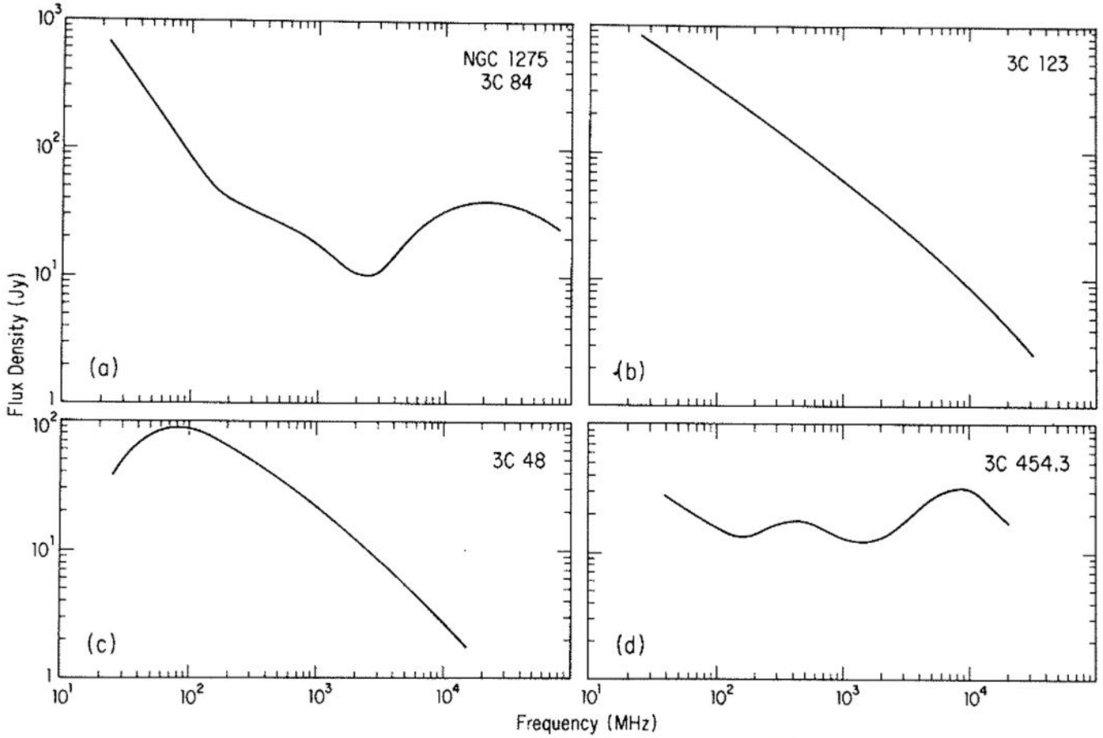

Figure 5.8: Representative spectra of radio galaxies and quasars [111]. The radio source 3C 84 in the nearby galaxy NGC 1275 contains a very compact nuclear component that is opaque below about 20 GHz. The radio galaxy 3C 123 is transparent at all plotted frequencies, and energy losses steepen its spectrum above a few GHz. The quasar 3C 48 is synchrotron self-absorbed only below 100 MHz, while the quasar 3C 454.3 contains structures of different sizes that become opaque at different frequencies.

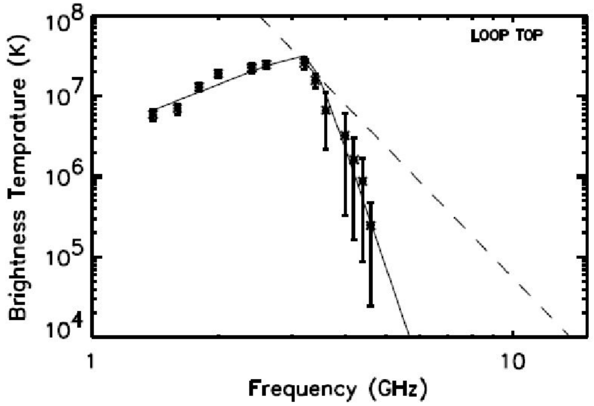

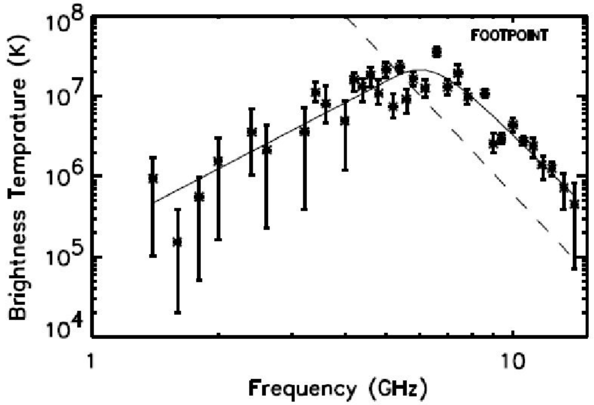

Wang et al. (1994)

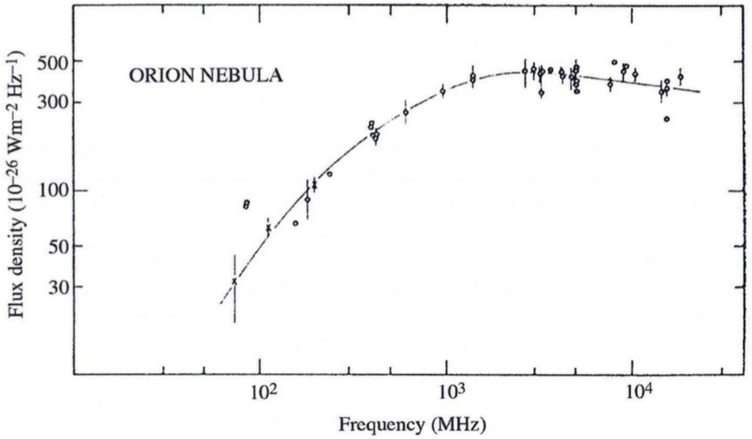

Figure 2.8. The spectrum of the observed radio emission from the Orion Nebula M42, showing the effect of increasing optical thickness at lower radio frequencies (after Terzian and Parrish 1970).

Credit: Unseen cosmos

ASTRON

DIAS
Institiúid Ard-Léinn Bhaile Átha Cliath | Dublin Institute for Advanced Studies

This project has received funding from the European Union's Horizon 2020 research and innovation programme under grant agreement No 952439.

STELLAR
Scientific and Technological Excellence by Leveraging LOFAR Advancements in Radio Astronomy

INSTITUTE OF ASTRONOMY NATIONAL ASTRONOMICAL OBSERVATORY

Selected links

https://www.famousscientists.org/how-hertz-discovered-radio-waves/

http://www.bigear.org/CSMO/HTML/CS12/cs12p08.htm

http://www.bigear.org/CSMO/HTML/CS13/cs13p14.htm

https://www.secretsofuniverse.in/karl-jansky/

https://web.njit.edu/~gary/728/Lecture2.html

https://suli.pppl.gov/2021/course/IntroToPlasma_Matthews2021.pdf

https://courses.engr.illinois.edu/ece350/PlasmaFormulary.pdf

Jasson Hessel, Lecture, 2013

ASTRON

DIAS
Institiúid Ard-Léinn Bhaile Átha Cliath | Dublin Institute for Advanced Studies